Full title:

Sex differences in change-of-mind neuroeconomic decision-making is modulated by LINC00473 in medial prefrontal cortex

Short title:

Neuroeconomic decision-making in males and females

Authors:

Romain Durand-de Cuttoli[1], Orna Issler[2], Benjamin Yakubov[3], Nusrat Jahan[3], Aisha Abid[3], Susanna Kasparov[3], Kastalia Granizo[3], Sanjana Ahmed[3], Scott J. Russo[1], Eric J. Nestler[1,4], Brian M. Sweis*[1,4]

*Corresponding: brian.sweis@mountsinai.org

Affiliations:

[1] Nash Family Department of Neuroscience, Friedman Brain Institute, Icahn School of Medicine at Mount Sinai, New York, NY 10029

[2] Neuroscience Institute, Department of Anesthesiology, Perioperative Care and Pain Medicine, and Department of Neuroscience and Physiology, NYU Langone, New York, NY 10016

[3] CUNY Hunter, New York, NY 10023

[4] Department of Psychiatry, Icahn School of Medicine at Mount Sinai, New York, NY 10029

Abstract:

Changing one's mind is a complex cognitive phenomenon involving a continuous re-appraisal of the trade-off between past costs and future value. Recent work modeling this behavior across species has established associations between aspects of this choice process and their contributions to altered decision-making in psychopathology. Here, we investigated the actions in medial prefrontal cortex (mPFC) neurons of long intergenic non-coding RNA, LINC00473, known to induce stress resilience in a striking sex-dependent manner, but whose role in cognitive function is unknown. We characterized complex decision-making behavior in male and female mice longitudinally in our neuroeconomic foraging paradigm, Restaurant Row, following virus-mediated LINC00473 expression in mPFC neurons. On this task, mice foraged for their primary source of food among varying costs (delays) and subjective value (flavors) while on a limited time-budget during which decisions to accept and wait for rewards were separated into discrete stages of primary commitments and secondary re-evaluations. We discovered important differences in decision-making behavior between female and male mice. LINC00473 expression selectively influenced multiple features of re-evaluative choices, without affecting primary decisions, in female mice only. These behavioral effects included changing how mice (i) cached the value of the passage of time and (ii) weighed their history of economically disadvantageous choices. Both processes were uniquely linked to change-of-mind decisions and underlie the computational bases of distinct aspects of counterfactual thinking. These findings reveal a key bridge between a molecular driver of stress resilience and psychological mechanisms underlying sex-specific decision-making capabilities.

41 **Introduction:**

42

43 How an individual changes one's mind when making choices is a challenging yet important
44 phenomenon that has been gaining more traction recently in the field of decision science [1]. This mental
45 process involves complex interactions between cognitive and affective systems and presents an
46 opportunity to peer into how the brain represents internal conflict [2, 3]. This captures conflict at multiple
47 levels, including the economic level: between competing interests of managing ongoing expenditures while
48 minimizing potential losses vs. maximizing future gains [4], as well as the psychological level: re-evaluating
49 one's own recent actions, which could be perceived as egodystonic [5-7]. Aspects of these processes are
50 likely dysfunctional in neuropsychiatric illnesses and may manifest as the cognitive changes observed in
51 mood disorders like depression, considering these mental operations could contribute to affective burden
52 [8, 9]. While the neural mechanisms underlying change-of-mind decision-making remain underexplored,
53 expanding this line of investigation holds promise to enrich our understanding of the repertoire of behavioral
54 processes at play in depression.

55

56 Depression is a debilitating mental illness characterized by pervasive mood disturbances, altered
57 cognitive capabilities, and maladaptations in motivated behavior [9]. The incidence of depression is two
58 times higher in women than in men and can manifest different symptomatology, including negative
59 rumination [10]; however, the molecular mechanisms mediating these sex differences are unclear [11-15].
60 Progress is being made toward appreciating neuroanatomical and pathophysiological differences between
61 depressed males and females based on advances in clinical and preclinical research, with the latter
62 enabling mechanistic studies of sex as a biological factor [16, 17]. Such advances are also due to adopting
63 novel approaches that leverage unsupervised analyses of large datasets in emerging fields of systems
64 biology leading to breakthroughs, for example, in identifying key regulatory roles of non-coding elements of
65 the genome [18].

66

67 Recent transcriptomics work carried out in human postmortem brain tissue samples obtained from
68 subjects carrying a diagnosis of major depressive disorder discovered sex-dependent functions of a

primate-specific long intergenic non-coding RNA: LINC00473 [19]. Overall, long non-coding RNAs represent a significant percentage of all of the regulated transcripts in human depression and are regulated in a sex- and brain region-specific manner. [19]. Lower LINC00473 expression levels were found in the medial prefrontal cortex (mPFC) of depressed females only [19]. Cross-species validation studies in rodents demonstrated expressing LINC00473 in mPFC neurons promotes resilience to stress in females only [19]. This included ameliorating depressive- and anxiety-like behaviors while blunting hypothalamic-pituitary-adrenal-axis activity as well as the induction of gene expression changes induced by chronic stress [19]. Other studies have implicated LINC00473 in molecular scaffolding, inter-organelle communication, and transcriptional regulation in non-neuronal tissue, while exhibiting immediate early gene-like properties in cultured neurons [20-25]. Beyond this, LINC00473 has not been studied in neural tissue in any other capacity, with no work performed to date on the role of long non-coding RNAs in regulating decision-making information processing.

Strides made in the field of neuroeconomics, an area focused on understanding how the brain is comprised of multiple valuation algorithms, have leveraged complex approaches in decision neuroscience to quantify how circuits constrain behavior [26-29]. This encompasses characterizing multifactorial aspects of motivation that operationalize reward value along several dimensions, integrate choice processes with environmental circumstances, and segregate stages of a decision into its component parts [30-33]. This work includes isolating properties of change-of-mind re-evaluative decisions, and points to the mPFC as a critical hub for regulating reward value, self-control, and mood [4, 34-38]. Insights from neuroeconomic principles offer novel approaches to investigate decision-making capable of resolving behavior into discretely measurable computational units in a manner that is biologically tractable and readily translatable across species [30, 39, 40]. This approach has yielded efforts from our team and others developing innovative tasks adapted for use in mice, rats, monkeys, and humans [5, 41-44]. The use of these translational tasks have led to cross-species discoveries uncovering the behavioral underpinnings of signatures of higher-order cognitive processes, previously thought to be unique to humans, supported by physically separable circuits in the brain [45-49].

Here, we characterized complex decision-making behavior in mice tested on our longitudinal neuroeconomic foraging paradigm, Restaurant Row. This task has been utilized previously to gain access to behavioral and neurophysiological correlates of multiple decision-making systems in the brain, including fundamentally distinct valuation algorithms engaged within the same trial [5, 47, 50-55]. On this task, rodents forage for their primary source of food among varying costs (delays cued by tone pitch) and subjective value (flavors tied to spatially fixed and contextualized locations, or “restaurants”) while on a limited time-budget. Decisions to accept and wait for rewards are separated into discrete stages of primary commitment (accept vs. reject in an offer zone) and secondary re-evaluation (stay vs. quit in a wait zone). We tested both male and female mice – the first ever analysis of females in this task – transfected with a newly packaged adeno-associated virus expressing LINC00473 or only a green fluorescent protein targeted mPFC neurons (**Supplementary Fig. 1**). Mice were tested daily over two months across a changing economic landscape during which complex foraging strategies developed. We report sex- and LINC00473-dependent differences in neuroeconomic decision-making behavior specific to alterations in multiple features of change-of-mind re-evaluative choices without affecting primary decisions. Differences were rooted in dissociable forms of counterfactual thinking, or how sensitive individuals were to missed opportunities for alternative actions that could have led to hypothetically better outcomes – the computational basis of regret processing previously captured by leveraging this task across species [5, 45, 46, 48, 56, 57].

115 **Results:**

116

117 *Male and female mice similarly acquire the Restaurant Row task.*

118 During the first week of Restaurant Row testing, all reward offers were fixed at 1 s only as mice
119 acquired the basic structure of the task (**Fig. 1a-b**), learning to run in the correct direction to forage for low-
120 cost food rewards. All mice were food restricted to the same percentage (~80-85%) of baseline free-feeding
121 weight (**Supplementary Fig. 2**). Both males and females, regardless of GFP or LINC00473 treatment,
122 grossly traveled similar total distances across the first week (**Fig. 1c**, sex*virus: F=0.971, p=0.331).
123 Behavior shaped equally among all groups as the number of laps run in the correct direction (**Fig. 1d**, day:
124 F=334.219, p<0.0001; sex*virus: F=2.780, p=0.104) and total pellets earned (**Fig. 1e**, day: F=393.991,
125 p<0.0001; sex*virus: F=3.062, p=0.089) increased across the first week. All mice displayed subjective flavor
126 preferences, revealed by splitting earnings by flavors ranked from least to most preferred by summing end-
127 of-session totals in each restaurant (**Fig. 1f**, rank: F=255.250, p<0.0001). There was a modest upward shift
128 in earns split by flavor ranking in LINC00473-treated females across the first week (**Fig. 1f**, sex*virus:
129 F=3.334, p=0.076). Overall, these data indicate all groups were able to demonstrate the ability to forage for
130 food in a self-paced manner without overt locomotor or feeding changes.

131

132 *LINC00473 alters value-dependent, task-driven conditioned place preference behavior in females.*

133 Before and after the first week of behavioral testing, we characterized exploratory behavior in the
134 maze arena (**Fig. 2a**). That is, without any task, mice were allowed to roam the maze freely on day 0 and
135 again on day 8 of the experimental timeline (**Fig. 2b**). This allowed us to probe a conditioned place
136 preference (CPP) response for reward sites driven by experience that naturally developed throughout the
137 first week of self-paced task performance. We measured the number of entries into and time spent near
138 the feeder site in each restaurant's wait zone on the probe sessions (**Fig. 2c**). All mice explored the arena,
139 including each restaurant, to similar degrees at baseline (day 0) and did not differ between groups
140 (sex*virus [entries]: F=0.259, p=0.614; sex*virus [time]: F=1.155, p=0.290, **Fig. 2c**). Overall, compared to
141 the day 0 pre-test baseline, we found that during the day 8 post-test all mice robustly increased total time
142 spent (F=75.818, p<0.0001) and to a lesser degree entries into the reward sites F=8.501, p<0.01, **Fig. 2c**).

143 We then split these metrics by restaurant ranked according to day 7's task earnings and found that CPP
144 scores scaled with flavor preferences (rank [entries]: F=16.307, p<0.0001; rank [time]: F=9.829, p<0.0001,
145 **Fig. 2d-e**). We found a significant decrease in CPP scores with respect to time spent in the wait zone of
146 the most preferred flavor in LINC00473-treated females only, despite being matched to males for equivalent
147 number of rewards earned on day 7 (sex*virus*rank [time]: F=2.844, p<0.05, **Fig. 2d-e**). This sex-
148 dependent effect was replicated in an independent cohort of mice separately transfected with a lower titer
149 of the AAV-expressing LINC00473 (**Supplementary Fig. 3**). Conversely, LINC00473-treated females
150 displayed an increased number of entries into less preferred restaurants compared to males or GFP
151 controls (sex*virus*rank [entries]: F=5.584, p<0.001, **Fig. 2d-e**, **Supplementary Fig. 3**). These findings
152 highlight that mPFC LINC00473 expression can have sex-specific effects on select actions during value-
153 based reward-seeking behavior. More specifically, LINC00473 treatment in females altered preferences-
154 dependent entering vs. exiting choices that may access dissociable computations involved in checking-
155 waiting-leaving behavioral sequences [51, 58, 59], shedding light on more precise interpretations of CPP
156 metrics than are traditionally reported and explored in detail below.
157
158 *Escalating reward scarcity unmasks sex-dependent effects of LINC00473 on complex foraging profiles.*
159 We next examined task foraging profiles across the subsequent weeks as we increased the
160 distribution of offer costs available in the task environment without adjusting the limited time budget mice
161 had to forage for food (**Fig. 3a**). Thus, in this closed-economy system, tightening budget constraints
162 pressured animals to adapt to the changing landscape of the environment as reward scarcity increased –
163 a model of economic stress we characterized recently [33]. Costs increased in a stepwise manner across
164 blocks of days (i.e., offers ranged from 1-5 s on days 8-12, 1-15 s on days 13-17, and finally 1-30 s on days
165 18-45, as previously published [5, 33, 60]) and were randomly sampled from a uniform distribution. As
166 expected, we found a decrease in pellets earned in response to each stepwise economic challenge (sign
167 test [-]: t=-12.655, p<0.0001, **Fig. 3b**). These deficits scaled by flavor and were matched between all groups
168 (rank: F=6.938, p<0.001, timepoint*rank: F=3.651, p<0.01; sex*virus: F=0.016, p=0.899, **Fig. 3c-d**,
169 **Supplementary Fig. 4**). The most striking change in behavior that accounted for environmental scarcity-
170 induced reward deficits across the experiment was the proportion of session time re-allocated to quitting

behavior in the wait zone, which significantly increased at each economic challenge step and more prominently in females (timepoint*choice: F=226.523, p<0.0001; timepoint*sex [quits]: F=11.821, p<0.0001, **Fig. 3e**, **Supplementary Fig. 4**). Across the final epoch of testing (the 1-30 s offer range period: days 18-45), mice displayed a complex response profile, including running more laps that developed over multiple weeks in an effort to recover and increase total food earnings (laps [days 18-45]: F=355.340, p<0.0001; earns [days 18-14]: F=252.218, p<0.0001, **Fig. 3b-d**). All groups were matched in their ability to recover earnings (sex*virus: F=0.234, p=0.631, **Fig. 3d**, **Supplementary Fig. 4**). However, we found that females displayed a greater increase in the number of laps run compared to males throughout this process (sex*day: F=7.848, p<0.01, **Fig. 3b**,**f**, **Supplementary Fig. 4**). Interestingly, LINC00473-expressing females displayed a significantly higher propensity to engage in wait zone quitting behavior compared to males that persisted across the entire experiment (sex*virus: F=8.201, p<0.01, **Fig. 3g**, **Supplementary Fig. 5**). Furthermore, LINC00473-expressing females displayed shorter latencies to quit upon arrival once in the wait zone compared to males particularly for more preferred flavors (sex*virus*day*rank: F=2.805, p<0.05), despite no changes in offer zone reaction times (F=1.713, p=0.162, **Supplementary Fig. 5**). Taken together, these data reflect rearrangements in complex foraging patterns that emerged across longitudinal time scales in response to worsening economic demand. These analyses reveal sex-dependent effects of mPFC LINC00473 expression that alter quit decisions unmasked in a reward-scarce environment. This effect of LINC00473 is reminiscent of the altered check-then-leave behaviors in LINC00473-expressing females during the CPP probe session (see Fig. 2)

Females demonstrate unique neuroeconomic decision-making policies during change-of-mind choices.

To characterize the economic nature of the decisions made during distinct action-selection processes in the offer zone and wait zone, we quantified choice outcomes to enter vs. skip (offer zone) or earn vs. quit (wait zone) separated by both the cued offer cost and flavor identity (**Fig. 4a-c**). All mice acquired the economic structure of the task, making cost-informed enter vs. skip choices in the offer zone or earn vs. quit choices in the wait zone, discriminating tones as well as demonstrating different degrees of willingness to wait in each restaurant (offer*flavor [offer zone]: F=13.129, p<0.001; offer*flavor [wait zone]: F=18.006, p<0.001, **Fig. 4a-c**). Thresholds of willingness to accept and separately wait for offers can be

199 calculated independently in the offer zone and wait zone by fitting a Heaviside step regression to the choice
200 outcome as a function of cost and extracting the inflection (indifference) point in each restaurant (**Fig. 4d**).
201 Overall, in all mice, we found that offer zone and wait zone thresholds significantly differed from each other
202 in magnitude of response to the changing economic landscape (timepoint*zone: F=296.648, p<0.0001, **Fig.**
203 **4d**). Upon transitioning to the 1-30 s epoch of testing (day 18), offer zone thresholds drastically increased
204 in all groups to similar degrees while retaining the ordinal ranking of flavor preferences (rank: F=17.247,
205 p<0.0001; sex: F=0.170, p=0.681; sex*virus: F=0.031, p=0.861, **Fig. 4d-f**). Wait zone thresholds, on the
206 other hand, increased only in male mice following the transition to the 1-30 s epoch (rank: F=58.574,
207 p<0.0001; sex: F=17.776, p<0.0001; sex*virus: F=1.238, p=0.268, **Fig. 4d-f**). Over the subsequent week
208 (days 18-24), wait zone thresholds in males decreased before stabilizing across the remainder of the
209 experiment (days 25-45, **Fig. 4d-f**). In females, wait zone thresholds remained relatively unchanged upon
210 transition to day 18 and were significantly lower than males across the entire 1-30 s epoch (sex*rank [offer
211 zone]: F=0.484, p=0.694; sex*rank [wait zone]: F=3.689, p<0.05, **Fig. 4d-f**). Offer zone thresholds on the
212 other hand gradually decreased, equally in all groups, but across a much slower timescale over several
213 weeks (**Fig. 4d-f**). Leveraging an economic analysis we recently developed [33], we found that female
214 decision-making policies were more optimized for both recovering food as well as yielding subjective value
215 in a reward-scarce environment (**Fig. 4g-i**, **Supplementary Fig. 6**). LINC00473 expression in mPFC did
216 not significantly alter any decision-making thresholds (sex*virus [offer zone]: F=1.781, p=0.185; sex*virus
217 [wait zone]: F=187, p=0.175, **Fig. 4d-f**). These data highlight a robust sex difference between distinct offer
218 zone and wait zone decision-making processes that we previously demonstrated derive from separable
219 circuits [48, 50].
220
221 *LINC00473 in mPFC enhances change-of-mind contrast via sensitivity to sunk costs and action-specific*
222 *regret.*
223 Wait zone thresholds capture economic indifference points of re-evaluation decisions defined by
224 choice outcome as a function of the starting offer. Next, we quantified more dynamically at what timepoint
225 quit decisions were made. Thus, we calculated the value remaining in the countdown at the moment of
226 quitting by subtracting the within-trial time remaining from an individual mouse's wait zone threshold (**Fig.**

227 **5a**). We found all mice generally made quit decisions: (i) for offers that were typically above one's wait zone
228 threshold (i.e., negatively valued offers) and (ii) with ample time remaining in the countdown such that the
229 time investment required to obtain the reward was still above one's threshold (i.e., negative value left), and
230 therefore would be advantageous to quit (**Fig. 5a**). Thus, overall, quit decisions reflected economically
231 advantageous re-evaluations of sub-optimal offer zone decisions relative to one's own policy, consistent
232 with previous reports [5, 33, 48, 49, 51]. We found that females made quit decisions with significantly lower
233 value remaining in the countdown compared to males (sex*virus: F=195.823, p<0.0001, **Fig. 5b**). This sex
234 difference was more pronounced in LINC00473-expressing animals and thus made females even more
235 efficient compared to males (sex*virus: F=12.957, p<0.001, **Fig. 5b**). Furthermore, only LINC0047-
236 expressing mice revealed a sex difference in the number of quit decisions that could be characterized as
237 economically advantageous (as described above, sex*virus: F=153.236, p<0.0001), with a greater
238 proportion in females compared to other quit events that were less common and more disadvantageous
239 (i.e., quitting negatively valued offers [above one's threshold] with positive value left [below one's threshold];
240 or, quitting positively valued offers [below one's threshold] – both reflecting quits passing the timepoint after
241 which mice should have chosen to stay instead (quit type*sex*virus: F=13.293, p<0.0001, **Fig. 5c-d**).
242
243 We then characterized the temporally dynamics of how mice made continuous re-evaluation
244 decisions in the wait zone as a function of the passage of time. We calculated the probability of staying and
245 earning a reward as a continuous function of not only (i) the time remaining in the countdown but also (ii)
246 the time already spent waiting. We computed a survival analysis using a sliding 1 s window after binning
247 all trials of varying starting offers into [time spent, time left] pairs (**Fig. 5f**). In all groups, we found that the
248 passage of time drove an increased likelihood that mice would continue to wait, the effect of which grew
249 additively stronger with escalating time spent (time spent*time left: F=891.924, p<0.0001, **Fig. 5f-h**). This
250 captures a well-studied cognitive phenomenon known as the sunk cost bias whereby irrecoverable past
251 expenditures can enhance the value of continuing to invest in and perseverate on an ongoing endeavor, as
252 we have reported previously across species [46, 49]. We found a significant sex difference in sensitivity to
253 sunk costs only in LINC00473-expressing mice. LINC00473-expressing females demonstrated increased
254 sensitivity to sunk costs compared to LINC00473-expressing males which instead demonstrated relatively

255 diminished sensitivity to sunk costs during quit decisions (sex*virus: F=15.944, p<0.0001, **Fig. 5i**). This
256 effect was independent of and orthogonal to temporal distance to the goal measured at any given moment
257 in time (**Fig. 5f**), only emerged after mice transitioned to the 1-30 s reward-scarce environment (time spent
258 in wait zone [1-15 s offers]: F=0.174, p=0.677, **Fig. 5i**, **Supplementary Fig. 7**), and uniquely affected wait
259 zone decisions compared to other forms of time spent on this task (time spent in offer zone: F=0.558,
260 p=0.455; time spent*sex*virus: F-0.418, p-0.518, **Supplementary Fig. 7**). These data highlight sex- and
261 LINC00473-dependent alterations in how the passage of time can differentially enhance reward value and
262 escalate the commitment to an ongoing endeavor specifically during re-evaluation decisions.
263
264 Next, we aimed to characterize how events related to quit decisions on a given trial influenced
265 subsequent behavior. Because trials are interdependent, a strength of the Restaurant Row task lies in being
266 able to subdivide trial sequences into unique economic scenarios in which animals naturalistically find
267 themselves. Analysis of mice after they make suboptimal choices and realize or gain access to information
268 that an alternative, unselected action could have led to a better outcome has led to breakthrough
269 discoveries modeling aspects of the behavioral and neurophysiological signatures of counterfactual thinking
270 – the computational basis of regret processing [5, 47, 48, 61-63]. We previously linked such processes to
271 quit decisions as well as other types of choices on this task [5, 47, 48]. In past reports, we and others
272 behaviorally operationalized counterfactual sensitivity on Restaurant Row by identifying trial pair sequences
273 [trial t-1 → trial t] in which animals made suboptimal choices [on trial t-1] and by measuring the change in
274 behavior on the next trial [on trial t: the read-out trial] [5, 47, 48]. Importantly, these events are compared
275 to specific control sequences that remove the error of one's own agency [on trial t-1], matched for all other
276 economic factors (e.g., including the offer values and flavor identities on both trials t-1 and trial t) in order
277 to behaviorally measure counterfactual sensitivity based on one's choice history. Recent work
278 demonstrated the importance of the mPFC in these behavioral responses [48]. Sequences were extracted
279 post hoc from natural encounters while foraging amid randomly presented offers, not constructed a priori
280 nor built into the task design.
281

We previously defined two distinct regret-related sequences of events on this task [5, 47, 48]. **Scenario 1**: situations in which animals inappropriately forgo a high-value offer [on trial t-1] only to subsequently encounter a worse low-value offer on the next trial [trial t] (**Fig. 5j**). This violation sequence can be compared to the non-violation control sequence in which mice instead appropriately accepted the high-value offer on trial t-1, holding all other variables constant (**Fig. 5j**). Here, we found that all groups were insensitive to scenario 1, with no effect of sex or LINC00473 expression (+ sign test: [male GFP]: t=-0.282, p=0.608; [female GFP]: t=0.101, p=0.461; [male LINC]: t=0.521, p=0.308; [female LINC]: t=-0.144, p=0.556, **Fig. 5j**). That is, there were no changes in behavior on the read-out trial when comparing violation sequences to non-violation sequences [thus yielding a delta score of zero in change of choice probabilities on trial t] (**Fig. 5j**). **Scenario 2**: situations in which animals inappropriately accepted a low-value offer [on trial t-1] that typically precipitates a resultant change-of-mind decision (**Fig. 5k**). This violation sequence can be compared to the non-violation control sequence in which mice instead appropriately skipped the low-value offer on trial t-1, holding all other variables constant and matched for the same low-value offer on trial t as in scenario 1 (**Fig. 5j-k**). Overall, we found that mice demonstrated sensitivity to scenario 2, whereby individuals were more likely to compensate for and accept low-value offers that they typically would not on the read-out trial following violation sequences compared to non-violation sequences (**Fig. 5k**). Interestingly, only GFP-treated females did not display scenario 2 sensitivity, while all other groups including LINC00473-expressing females displayed delta scores significantly greater than zero (+ sign test: [male GFP]: t=2.931, p<0.01; [female GFP]: t=1.123, p=0.145; [male LINC]: t=3.056, p<0.01; [female LINC]: t=2.196, p<0.05, **Fig. 5k**). Taken together, these data reveal how mice can differentially carry the weight of different types of past mistakes into future choices, with a unique association between change-of-mind-related counterfactual sensitivity and mPFC LINC00473 expression in females. These findings provide an example whereby LINC00473 expression in this brain region overcomes a baseline sex difference that normally disadvantages females.

Lastly, we characterized how access to task-relevant information may be critically important for sex- and LINC00473-dependent differences during change-of-mind decisions. After day 45, we tested mice for an additional 2 days during which tone playback was silenced only in the wait zone but remained audible

310 during offer zone presentations (**Fig. 6a**). That is, mice had access to cost information signaled by tone
311 pitch when making initial enter vs. skip decisions in the offer zone, but received no countdown information
312 once in the wait zone while making secondary re-evaluative decisions to quit or stay before earning
313 rewards. Overall, we found that males were more sensitive to this informational manipulation compared to
314 females. Both GFP- and LINC00473-expressing males displayed a modest decreased number of laps run
315 and total number of pellets earned, while female mice remained relatively unchanged between audible and
316 silent conditions (laps [timepoint*sex]: F=10.678, p<0.01; laps [timepoint*virus]: F=0.449, p=0.507; earns
317 [timepoint*sex]: F=10.124, p<0.01; earns [timepoint*virus]: F=0.002, p=0.969, **Fig. 6b-c**). This task
318 manipulation did not alter any overt changes in offer zone choices in any group as animals continued to
319 discriminate the audible tones during cost-informed enter vs. skip decisions (offer: F=1186.818, p<0.0001;
320 offer*timepoint: F=1.365, p=0.243; **Fig. 6d**). Interestingly, when examining changes in wait zone thresholds,
321 we found a significant sex difference that was compounded by an additional LINC00473 effect in females
322 only (**Fig. 6e**). In males, compared to the audible condition, the lack of auditory information cuing mice on
323 progress during the countdown in the silent wait zone condition drove an increase in wait zone thresholds
324 for most preferred flavors (timepoint: F=22.976, p<0.0001; timepoint*virus: F=0.181, p=0.671 **Fig. 6e**).
325 Males also displayed a concomitant decrease in wait zone thresholds for least preferred flavors (timepoint:
326 F=19.561, p<0.0001; timepoint*virus: F=0.526, p=0.470, **Fig. 6e**). These data indicate that, without cued
327 auditory guidance in the wait zone, males were more patient waiting for favorite flavors and less patient
328 waiting for least favorite flavors. Conversely, GFP-expressing females only displayed a decrease in wait
329 zone thresholds for less preferred flavors, with no change in thresholds for most preferred flavors (**Fig. 6e**).
330 LINC00473-expressing females however did not display any changes in wait zone thresholds in any
331 restaurant between audible and silent wait zone conditions (timepoint [most preferred]: F=2.569, p=0.112;
332 timepoint*virus [most preferred]: F=0.137, p=0.712; timepoint [least preferred]: F=12.185, p<0.0001;
333 timepoint*virus [least preferred]: F=8.901, p<0.01). These data indicate LINC00473-expressing females
334 valued offers in a consistent manner with or without externally guided information, suggesting that their
335 internal measures of time or holding information from the offer zone in working memory may be more stable.
336 When examining quit times in the wait zone, all mice displayed a modest increased latency to quit in the
337 silent condition compared to the audible condition (timepoint: F=11.764, p<0.001; sex: F=2.358, p=0.126;

338 virus: F=0.836, p=0.361, **Fig. 6f**). Finally, when examining sensitivity to sunk costs, we found that the silent
339 condition unmasked a sex difference in GFP-treated mice whereby females show increased sensitivity as
340 a function of the passage of time compared to males that was previously only apparent in LINC00473-
341 expressing groups during the audible condition (time spent: F=97.196, p<0.001; sex: F=36.989, p<0.0001;
342 virus: F=1.899, p=0.168; **Fig. 6g**, see **Supplementary Fig. 8** for alternate task information manipulations).
343 Taken together, these findings highlight the complexity of change-of-mind decisions, how mice internally
344 generate value representations with vs. without access to explicit task-relevant information, and the
345 multifactorial ways in which this re-evaluative choice process can be uniquely modulated in a sex-
346 dependent manner.

347 **Discussion:**

348

349 In this study, we characterized highly complex behavior in mice tested on the neuroeconomic
350 foraging paradigm, Restaurant Row. We explored the role of a non-coding RNA, a relatively poorly
351 understood class of molecules, on motivated behavior. We discovered sex-dependent effects of LINC00473
352 expression in mPFC neurons on specific aspects of value-based decision-making information processing.
353 This was typified by selectively altering the way in which an individual changes one's mind during an
354 ongoing decision. Importantly, we discovered a role for mPFC LINC00473 expression – which increases
355 stress resilience in simple behavioral screening tests in female mice only [19] – in sharpening the contrast
356 of re-evaluation processes in females. Our findings extend from simple conditioned place preference
357 behaviors like those commonly assayed using simpler paradigms [40, 64, 65] to more complex, higher order
358 neuroeconomic phenomena. These latter effects included enhancing specific aspects of sensitivity to sunk
359 costs and counterfactual thinking. These data provide a better understanding of how multiple stages of a
360 continuous decision stream derive from dissociable psychological mechanisms supported by physically
361 separable circuits in the brain. Our findings have important implications for how molecular determinants of
362 stress responses influence changes in motivated behavior via unique decision-making computations
363 differentially leveraged by males and females.

364

365 The distinction between offer zone choices and wait zone choices on the Restaurant Row task is
366 critically important. They reflect a separation of fundamentally distinct decision-making algorithms that occur
367 within the same trial but are segregated across space and time [51]. Numerous reports have tested subjects
368 on this paradigm translated for use across species in task variants adapted for mice, rats, monkeys, and
369 humans [41, 42, 46]. These studies have shed light on the biological and psychological implications of
370 resolving dissociable, evolutionarily conserved decision-making processes. In the offer zone, individuals
371 engage deliberative systems that represent alternating options of competing actions between which one
372 must choose [54, 55]. This has been shown in rodents to derive in part from hippocampal (HPC)-dependent
373 processes [50, 51]. Population level activity of neurons in HPC is capable of decoding multiple, alternating
374 future paths through the offer zone to potential goals in the current vs. next restaurant [58, 64, 66, 67].

375 Similar findings have been observed from fMRI studies in humans tested on a translated version of the
376 Restaurant Row task [45]. Default mode network activation patterns can decode competing future options
377 during offer zone deliberation, but seldom do such representations include past events or previous
378 restaurants [2, 68]. Decisions in the wait zone on the other hand are much less understood. The HPC has
379 been implicated in wait zone decisions as well: it switches oscillatory activity from a predominately theta-
380 driven state sensitive to the cued offer costs in the offer zone [54] instead to an increase in sharp wave
381 ripple activity sensitive to time spent waiting in the wait zone [55]. Further, wait zone decision periods also
382 depend on HPC synchrony with the mPFC [54, 55]. Recordings in rodents from the mPFC surprisingly
383 found no evidence of encoding of the cued offer costs when animals were in the offer zone [52]. However,
384 once in the wait zone, mPFC neurons strongly represented offer value independent of time spent waiting
385 and could predict whether or not the trial would terminate in a quit [52]. Within the mPFC, pairs of neurons
386 also drastically changed excitation-inhibition balance specifically when animals were in the wait zone [69].
387 Taken together, these findings indicate a qualitative shift in mental state upon transition from the offer zone
388 to the wait zone that recruits the mPFC exclusively during change-of-mind decisions.
389
390 This study represents the first analysis of females in the Restaurant Row task. Nearly all of the sex
391 differences captured here, including those altered by mPFC LINC00473 expression, are restricted to wait
392 zone and not offer zone behaviors. Furthermore, sex differences not only persist but are even exaggerated
393 when access to task-relevant cost information is restricted in the wait zone during change-of-mind
394 decisions. We showed recently that LINC00473 expression diminishes spontaneous excitatory post-
395 synaptic current frequency and amplitude in excitatory mPFC pyramidal neurons of female mice, with no
396 effect seen in males [19]. Chemogenetic inactivation of the mPFC diminishes wait zone quit decisions [53-
397 55]. Optogenetic induction of long-term depotentiation in excitatory mPFC neurons that project to the
398 nucleus accumbens (NAc) [50], where negative deflections in dopamine signals have been found to
399 causally precede quit choices [70], selectively decreases quitting behavior for several days without altering
400 offer zone behavior [50]. Outside of Restaurant Row, intracranial optogenetic excitatory self-stimulation of
401 mPFC terminals in the NAc can be reinforcing while also promoting enter-then-quitting behavior [71]. These
402 converging findings suggest that LINC00473 expression is likely mediating sex-dependent effects on

403 change-of-mind decisions by at least in part dampening and restructuring mPFC activity. How these
404 alterations in change-of-mind decisions relate to mPFC LINC00473's known role in enhancing resilience to
405 stress in a sex-dependent manner will help bridge interpretations between molecular drivers of stress
406 responses and the behavioral computations associated with susceptibility vs. resilience to stress in males
407 and females.
408
409 Recent transcriptomic analyses of human postmortem mPFC obtained from individuals diagnosed
410 with major depressive disorder revealed a female-specific decrease in LINC00473 expression in the mPFC
411 [19]. While LINC00473 is not normally expressed in rodents – it arose in the primate lineage – expressing
412 LINC00473 in mouse mPFC neurons demonstrated pro-resilient effects in females, but not males,
413 protecting against several depressive-like phenotypes in simple behavioral tests after exposure to chronic
414 social defeat or variable stress [19]. LINC00473 expression, which predominates in pyramidal neurons in
415 human mPFC [19], has been shown to be regulated by conserved Ca^{2+}/calmodulin signaling pathways and
416 is likely induced by cAMP response element-binding protein (CREB) [19-21, 23]. CREB has long been
417 studied based on more traditional candidate gene approaches and shown to regulate numerous other
418 genes involved in neuronal excitability and synaptic plasticity as well as stress sensitivity [72-77]. Like
419 LINC00473, CREB function in the mPFC has been implicated in promoting resilience to stress, however,
420 unlike LINC00473, this has been shown to be true for both males and females [19, 78]. These reports
421 suggest either that there must be some divergence of intracellular CREB-LINC00473-interacting molecular
422 pathways between sexes conferring differential sensitivities to stress, or that prior studies were limited in
423 their ability to resolve more nuanced sex differences at the behavioral level.
424
425 We recently characterized the impact of chronic social defeat stress on Restaurant Row behavior
426 in male mice, in tandem with disruptions of CREB function in mPFC [33, 48, 79]. First, we found that male
427 mice were required to progress through worsening economic challenges in order to extract any group
428 differences in foraging profiles [33]. This is consistent with results presented here that emphasize the
429 importance of considering the environmental demand and stressors of a task. Second, we found that stress-
430 resilient mice – defined by a simple social interaction screening test – mounted the most robust behavioral

431 activation in response to the transition into the 1-30 s reward-scarce environment in efforts to recover and
432 maintain food security despite budget constraints, similar to LINC00473-expressing female mice as shown
433 here [33]. Third, without grossly altering decision-making thresholds, we found that stress-susceptible male
434 mice demonstrated increased regret-related sensitivity to type 1 scenarios (economically risky decisions to
435 skip, followed by poor outcomes), a phenotype no group demonstrated in the present study [48].
436 Additionally, stress-susceptible mice demonstrated diminished regret-related sensitivity to type 2 scenarios
437 (change-of-mind decisions) compared to stress-resilient individuals who instead displayed enhanced
438 change-of-mind sensitivity to both regret and sunk costs related to quitting behavior [48]. Interestingly, in
439 the present study, this constellation of differences was only apparent among the GFP-expressing and
440 LINC00473-expressing females, respectively, suggesting that females at baseline have a decision-making
441 vulnerability specifically in change-of-mind choice processes that is restored to male levels by LINC00473
442 expression in mPFC. In our earlier study, knocking down CREB function had multifactorial effects
443 depending on the neuroeconomic valuation algorithm in question, the brain region targeted (mPFC vs.
444 NAc), and whether or not animals were stress-naïve at baseline vs. exposed to subsequent stress [48].
445 CREB function in the mPFC was required to maintain suppression of regret-related sensitivity to type 1
446 scenarios and, when knocked down, rendered only type 2 scenarios sensitive to subsequent stress – a
447 response profile distinct from CREB function in the NAc where it is known to drive stress susceptibility [48,
448 72, 80, 81]. These data shed light on a divergence between CREB and LINC00473 in mediating dissociable
449 aspects of counterfactual thinking that could independently contribute to the affective toll of past mistakes
450 and one's overall mood burden. While these prior studies were conducted in males [33, 48, 79], they
451 highlight multiple dimensions with which to consider how information integrates across fundamentally
452 distinct choice processes in order to ultimately precipitate sex-dependent behavioral phenotypes related to
453 one's stress vulnerability.
454
455 LINC00473's sex-dependent effects on behavior have only been causally tested in the mPFC to
456 date [19]. Although postmortem human tissue studies implicate mPFC as a top region to investigate [19],
457 understanding LINC00473's role in other regions, especially in how it may be interacting with other key
458 molecular players such as CREB in the NAc [23, 72, 73], will be critically important in future studies to

459 elucidate how information processing integrates across neural networks. For instance, LINC00473 has
460 been shown to increase cellular excitability in cultured HPC neurons [23], contrary to its effects in mPFC
461 [19]. Future decision-making studies should combine experiments of LINC00473 manipulations with
462 exposure to other stressors, beyond the economic challenges tested in the present study, such as chronic
463 social defeat or variable stress to explore compounding effects [19]. Further, more work needs to be done
464 toward investigating the role of gonadal steroid hormones, sex chromosomes, and sex-dependent
465 noncoding RNAs in mediating aspects of the reported sex differences. As just one example, CREB function
466 has been shown to fluctuate with estrus cycle [82-86]. Additionally, given previous reports that LINC00473
467 expression in mPFC of stress-naïve male mice does induce behavioral changes in certain simpler assays
468 (i.e., marble burying) [19], it would be fruitful to explore in future work how Restaurant Row decision-making
469 profiles could potentially relate to individual differences in task-unrelated traits (e.g., anxiety-related
470 behavior measured on independent tests). Lastly, it is critically important to consider how the decision-
471 making processes as measured here could relate directly to and drive information processing during the
472 expression of one's symptomology itself (e.g., underlying the choices leading to anhedonia or social
473 avoidance related behaviors themselves) as opposed to occupying a more general role as a trait of the
474 individual.
475
476 Taken together, we discovered robust sex differences in the overall contrast of how an individual
477 decides to change one's mind. This is conceptualized as how dynamic a value representation can be when
478 deciding to quit an ongoing endeavor and the strength with which quitting behavior can influence the
479 psychology of multiple cognitive processes. We characterized this as both the steepness of a tipping point
480 during change-of-mind decisions to either stay or quit and the weight such events can carry into future
481 choices. We found that this lability depends on individual differences in one's subjective value, on the state
482 of the environment in the form of how scarce reward availability and access to information might be, and is
483 uniquely enhanced by LINC00473 expression in mPFC of females. Counterfactual thinking during change-
484 of-mind decisions can elicit "should not have done that" mental representations that map hypothetical
485 outcomes onto alternative actions that could have been selected instead. Even if change-of-mind decisions
486 are an unpleasant experience or evoke to some degree a form of cognitive dissonance, enhancing the

487 sharpness of this process could increase attention paid toward realized losses, can possess utility for fictive
488 learning, and collectively may be a sex-dependent feature of stress resilience altering the lens through
489 which individuals process their prior mistakes.

490 **Figure Captions:**

491

492 **Fig. 1 | Male and female mice acquire the Restaurant Row task. a** Experimental timeline. 40 C57BL/6J
493 mice (20 male, 20 female) underwent stereotaxic surgery, half of each sex receiving AAV-LINC00473 or
494 AAV-GFP viruses injected bilaterally in the mPFC. Mice were allowed to recover before beginning
495 longitudinal testing on the Restaurant Row task for 45 consecutive days. Dashed box indicates time period
496 relevant for this figure: week 1 of behavioral testing. **b** Task schematic. Mice were allotted 30 min daily to
497 invest time foraging for their primary source of food in a self-paced manner. Costs to obtain rewards were
498 in the form of delays mice would have to wait near feeder sites. Mice were required to run in a
499 counterclockwise direction encountering offers for different flavors at each "restaurant" in serial order. Each
500 restaurant, separated by hallways, was divided into a T-shaped "offer zone" choice point and a separate
501 "wait zone" that housed the pellet dispenser. Upon offer zone entry from the correct heading direction, a
502 tone sounded whose pitch indicated the delay mice would have to wait if accepting the offer by entering the
503 wait zone. If entered, tone pitch descended in the wait zone, cuing the indicated delay. Each trial terminated
504 if mice skipped in the offer zone, quit during the countdown in the wait zone, or earned a reward, after which
505 animals were required to proceed to the next restaurant. **c-f** Simple behavioral metrics across the first week
506 of testing during which all offers were 1 s only (lowest pitch, 4 kHz): (c) total distance traveled, (d) laps run
507 in the correct direction, (e) total rewards earned, (f) earnings split by flavors ranked from least to most
508 preferred by summing each day's end-of-session totals in each restaurant. No effect of sex or LINC00473
509 expression was grossly apparent in these initial metrics. Error bars represent ±1 SEM.

510

511 **Fig. 2 | LINC00473 expression in mPFC alters value-dependent, task-driven conditioned place**
512 **preference behavior in females. a** Experimental timeline. Dashed box indicates time period relevant for
513 this figure: two special testing days marked with cyan arrows. **b** Experimental design. Animals were placed
514 in the arena free to roam for 20 min on day 0 and day 8 of the experimental timeline but with no active task
515 to obtain pre-task baseline and post-task experience-related exploratory behavior. **c** Total number of entries
516 and total time spent in the wait zone, aggregated in all restaurants. **d-e** Delta scores in change of (d) total
517 entries and (e) total time comparing post (day 8) minus pre (day 0) time points split by restaurants ranked

518 according to rewards earned on the active task on day 7. Only the most preferred (1st) and least preferred
519 (4th, faint) restaurants are depicted here (see Supplementary Fig. 3 for full dataset and replication cohort).
520 Horizontal dashed gray line indicates delta score of 0. LINC00473 expression in mPFC abolished CPP
521 behavior in most preferred restaurants only in females and only in the time but not entry domain. *Represent
522 significant sex differences. Error bars represent ±1 SEM.
523
524 **Fig. 3 | Escalating reward scarcity unmasks sex-dependent effects of LINC00473 expression in**
525 **mPFC on complex foraging profiles. a** Experimental timeline. Dashed box indicates time period relevant
526 for this figure: the entire 45-day Restaurant Row paradigm. **b** Total rewards earned (black) and laps run in
527 the correct direction (gray). All 40 mice collapsed. Visual guidance color bars along the x-axis reflect the
528 experimental schedules of the change the distribution of offer costs illustrated in the timeline in (a). Vertical
529 dashed green-yellow-red lines indicate the transition points of the stepwise schedule of and are re-used
530 throughout all other figures as a visual aid. Inset depicts "hysteresis" plot of laps against earns (epochs of
531 days are color-coded). **c** Rewards earned split by flavors ranked from most preferred (1st) to least preferred
532 (4th, faint). All 40 mice collapsed. **d** Change in rewards earned in each restaurant comparing two days at
533 various color-coded transition points (delta scores calculated by subtracting the following: i, day 8-7
534 (yellow); ii, day 13-12 (orange); iii, day 18-17 (red); iv, day 45-18 (purple). All 40 mice collapsed (see
535 Supplementary Fig. 4 for comparison between groups). **e** The portion of total session time engaged in one
536 of the four major choice behaviors: offer zone – enter (green) or skip (red); wait zone – quit (magenta) or
537 earn (blue). Rings split restaurants ranked from most preferred (1st, inner ring) to least preferred (4th, outer
538 ring). Each of the 5 pie charts represent data from each stage of testing, with the early and late epochs
539 during the 1-30 s offer range extracted from the first 5 and last 5 days of that period. **f** Laps run in the correct
540 direction split by sex and treatment groups. **g** Proportion of enter decisions that terminated in a quit outcome
541 once in the wait zone. LINC00473 expression in mPFC drove females to run more laps in response to a
542 worsening economic landscape and quit more frequently. *Represent significant sex differences. Shading
543 / error bars represent ±1 SEM.
544

Fig. 4 | Females demonstrate unique neuroeconomic decision-making policies during change-of-mind choices. a Experimental timeline. Dashed box indicates time period relevant for this figure: the entire 45-day Restaurant Row paradigm. **b** Example behavior from a single mouse early or late during the final 1-30 s testing epoch (red portion of the experimental timeline). Data depict offer zone choice outcomes on the y-axis (enter vs. skip) as a function of the randomly presented cued offer cost (tone pitch) on the x-axis in each restaurant (dots represent individual trial choice outcomes). Quit outcomes in the wait zone are indicated in black dots. **c** Aggregate example summary choice data from all 40 mice early or late during the final 1-30 s testing epoch. Data depict separate offer zone or wait zone summary probability of choice outcome. Horizontal dashed gray line indicates chance at 0.5. Mirror curves for skip and quit (1-probabilities) are intended to highlight cross over points that approximate threshold fits. **d** Thresholds or indifference points of willingness to accept offers in the offer zone or earn offers in the wait zone. Inset depicts an example session from a single mouse in one restaurant where vertical solid green or blue lines illustrate the inflection of Heaviside-step regression fits to choice outcomes in each zone as a function of starting offer costs. All 40 mice collapsed. Inset depicts “hysteresis” plot of offer zone against wait zone thresholds (epochs of days are color-coded). **e** Offer zone thresholds (top) and wait zone thresholds (bottom) split by sex and treatment groups. GFP groups in faint dashed lines. **f** Thresholds from (e) extracted from early and late 1-30 s epoch (red). GFP groups in dashed lines. **g-i** Economic analysis of how well offer zone and wait zone decision policies during the 1-30 s epoch approximate subjective value yield as determined from individual differences in earnings by flavor acquired during the low-cost environment earlier in testing (day 7) when all rewards cost only 1 s. This is compared against theoretical decision policies that maximize total food intake during the 1-30 s epoch irrespective of flavor. See Methods and Supplementary Fig. 6 for a full explanation of this analysis. (g) Individual differences in (top) the standard deviation of rewards earned across flavors on day 7, (middle) total rewards earned on day 7, and (bottom) earns split by restaurant coded in color (flavor: chocolate-brown, banana-yellow, grape-purple, plain-cyan) and size (reward count) on day 7. All data in (g) is sorted by stdev data in (top). Small colored boxes along the x-axis indicate sex (male-blue, female-red) and treatment groups (LINC-dark, GFP-light). **h** Example data from a single mouse on day 7 showing value ratios among earns between restaurants relative to the least preferred flavor (faint). **i** Data from (g-h) used in a computational modeling analysis to

573 calculate the Euclidean distance between observed decision policies each day from days 18-45 (cool to
574 warm colors, each dot indicates group average per day) to theoretical policies that could achieve either
575 maximal food (x-axis) or maximal subjective value (y-axis) for offer zone and wait zone thresholds. Inset
576 diagonal lines indicate reference point for the 1:1 unity line. Prominent sex difference, without apparent
577 effect of LINC00473 expression in mPFC, in present in wait zone but not offer zone economic decision
578 policies. *Represent significant sex differences. Shading / error bars represent ±1 SEM.
579
580 **Fig. 5 | LINC00473 expression in mPFC enhances change-of-mind contrast via sensitivity to sunk**
581 **costs and action-specific regret. a** Distribution of quit trials as a function of offer value (x-axis) or value
582 left at the moment of quitting (y-axis) defined relative to one's wait zone threshold (origin vertical and
583 horizontal dashed blue lines). Data split by restaurants ranked from least to most preferred. All 40 mice
584 collapsed. Data extracted from the entire 1-30 s epoch. **b** Average value left at the moment of quitting split
585 by sex and treatment groups. Horizontal dashed gray line indicates 0 value left (or wait zone threshold). **c**
586 Three categories of quit events based on offer value and value left terms. The green quadrant ($V_o<0$ &
587 $V_L<0$) represent the most efficient quit decisions from economically disadvantageous offers. **d** Counts of
588 total number of quit events aggregated across all restaurants from each economic quit category described
589 in (c). **e** Counts of total number of quit events from each economic quit category in (d) split by restaurants
590 ranked from least (4th) to most preferred (1st) extracted from the entire 1-30 s epoch (red). **f-h** Sunk cost
591 analysis of staying behavior in the wait zone, demonstrated using all 40 mice. (f) The likelihood of staying
592 in the wait zone and earning a reward (e.g., not quit) is plotted as a function of time left in the countdown
593 along the x-axis and time already spent waiting orthogonally in color. Note the black 0 s time spent curve
594 represents animals having just entered the wait zone from the offer zone. Inset vertical dashed gray line
595 illustrates an example analysis point comparing three sunk cost conditions originating from different starting
596 offers but matched at 10 s left. Data from (f) dimensioned reduced in (g) collapsing across time left,
597 highlighting the grand mean of each time spent sunk cost condition (color and x-axis). Insets in (g) depict
598 data from curves in (f) are collapsed into the observed (sunk condition) and control (0 s condition) lines.
599 Difference between curves in (g) are plotted in (h) in order to summarize the envelope of the overall effect
600 of time already spent on escalating the commitment of staying in the wait zone. Horizontal dashed line

601 represents delta score of 0. **i** Sensitivity to sunk costs plotted across the entire Restaurant Row paradigm
602 where the delta curve in (h) is plotted as vertical slices in (i) with time already spent along the y-axis and
603 heatmap representing delta score magnitude. **j-k** Regret-related sequence analyses comparing trial pairs
604 between (j) type 1 scenarios and (k) type 2 scenarios each. Read out trials captures a change in behavior
605 depending on choice history of distinct economic violations (black) compared to non-violations (gray) on
606 trial t-1. Read out trials report delta scores in likelihood change of entering by subtracting choice outcomes
607 between violation-nonviolation sequences. Horizontal dashed gray line indicates delta score of 0. See
608 Methods for a full explanation of these analyses. Prominent sex-dependent effect revealed by LINC00473
609 expression in mPFC on change-of-mind related sunk costs (enhanced in females) and regret sensitivity
610 (type 2: enhanced in females). ***** in (b-i) represent significant sex differences. * in (j-k) represent delta score
611 significantly different from 0. Shading / error bars represent ±1 SEM.
612
613 **Fig. 6 | Sex- and LINC00473-dependent wait zone behaviors are differentially modulated by access**
614 **to task information. a** Informational manipulation schematic: (left) standard Restaurant Row task followed
615 by (right) two days of tones silenced only in the wait zone, but not offer zone (remains audible as before).
616 **b** Total number of laps run in the correct direction (top) and total pellets earned aggregated among
617 restaurants (bottom) across the audible and silent wait zone task conditions (x-axis). **c** Rewards earned in
618 each restaurant ranked from least (4th) to most preferred (1st) across the audible (black) and silent wait zone
619 (gray) task conditions. **d** Overall offer zone choice probabilities to make enter decisions as a function of
620 audible cued offer costs collapsed across all flavors to illustrate no effect of task condition on auditory
621 discriminatory behaviors. Horizontal dashed line indicates change at 0.5. **e** Wait zone thresholds in each
622 restaurant across task conditions. **f** Latency to quit reaction times once in the wait zone in each restaurant
623 across task conditions. **g** Sensitivity to sunk costs in the wait zone depicted here only in the silent condition
624 as a function of time already spent (x-axis). Y-axis reflects delta earn probabilities as depicted in Fig. 5h.
625 Prominent sex-dependent effects of withholding wait zone information on overall task performance
626 (observed in males), wait zone economic decision policies (bidirectional in males, unidirectional in GFP-
627 females, and no effect in LINC00473-females), and sunk cost sensitivity (sex difference revealed for the
628 first time GFP groups unlike in Fig. 5). Horizontal dashed line indicates delta score of 0. ***** in (b-f) represent

629 significant effects of task condition within group. * in (g) represent significant sex differences. Shading /

630 error bars represent ±1 SEM.

Acknowledgments:

We thank members of the labs of Eric Nestler and Scott Russo for helpful discussion and technical assistance. Open-source illustrations obtained from SciDraw (www.scidraw.io), credit Federico Claudi.

Funding:

National Institute of Mental Health grant R01MH051399 (EJN)
National Institute of Mental Health grant R01MH129306 (EJN)
National Institute of Mental Health grant R01MH114882 (SJR)
National Institute of Mental Health grant R01MH127820 (SJR)
National Institute of Mental Health grant R01MH104559 (SJR)
National Institute of Mental Health grant L40MH127601 (BMS)
National Institute of Mental Health supplement grant R01MH051399-31S1 (BMS)
Leon Levy Scholarship in Neuroscience, New York Academy of Sciences (BMS)
Burroughs Wellcome Fund Career Award for Medical Scientists (BMS)
Animal Models for the Social Dimensions of Health and Aging Research Network via NIH/NIA R24 AG065172 (BMS)
Brain & Behavior Research Foundation Young Investigator Award 31140 (RDC)

Author contributions:

Conceptualization: RDC, OI, EJN, BMS
Methodology: RDC, OI, BMS
Investigation: RDC, BY, NJ, AA, SK, KG, SA, SJR, EJN, OI, BMS
Data curation: RDC, OI, BMS
Formal analysis: BMS

Visualization: RDC, OI, BMS

Funding acquisition: OI, BMS

Supervision: RDC, BMS

Writing – original draft: RDC, OI, BMS

Writing – review & editing: RDC, BY, NJ, AA, SK, KG, SA, SJR, EJN, OI, BMS

Competing interests:

Authors declare that they have no competing interests.

Data and materials availability:

All data and materials used in the analysis are available in the manuscript, materials and methods section, or supplementary information.

673 **Supplementary Figure Captions**

674

675 **Supplementary Fig. 1 | Validation of newly packaged adeno-associated virus expression of**
676 **LINC00473.** Raw qPCR cycle threshold count (ct) obtain from mPFC tissue punches extracted from mice
677 separately transfected with either AAV2-hSyn-GFP (control) or AAV2-hSyn-LINC00473-GFP (treatment).
678 qPCR readouts obtained for expression levels of GFP, HPRT1 (housekeeping), ZFP189 (another known
679 regulator of stress-resilience), and LINC00473. Note similar levels of expression of GFP, HPRT1, and
680 ZFP189 between control and treatment viruses. Also note no detectable levels of LINC00473 in mice
681 transfected with the control virus, as this is not endogenously expressed in mice. Dots represent individual
682 samples. Error bars represent ±1 SEM.

683

684 **Supplementary Fig. 2 | Bodyweight measurements.** Percentage of a 2-day average (circled in gray,
685 horizontal dashed line for reference) of baseline body weight obtained 4 days prior (black epoch) to the
686 start of the longitudinal Restaurant Row paradigm. During this period (black epoch), mice were food
687 restricted and fed a limited ration to intentionally decrease weights to approximately 80-85% of baseline
688 that was steadily maintained throughout the remainder of the experiment (days 1-45, see main Fig. 1 for
689 an explanation of the color-coded epochs of testing across the paradigm). These body weights reflect the
690 measurements immediately before task performance on each day of testing. Shaded area represents ±1
691 SEM.

692

693 **Supplementary Fig. 3 | Replication cohort of two different virus titers on sex-specific Restaurant**
694 **Row conditioned place preference (CPP) findings.** Animals were placed in the arena free to roam for
695 20 min on day 0 and day 8 of the experimental timeline but with no active task to obtain pre-task baseline
696 and post-task experience-related exploratory behavior (see main Fig. 2). **a** Total number of entries and total
697 time spent in the wait zone, aggregated in all restaurants. Depicting findings from independent cohorts. **b**
698 Delta scores in change of entries and time comparing post (day 8) minus pre (day 0) time points split by
699 restaurants ranked according to rewards earned on the active task on day 7. **c** Data from (b, only 1st and
700 4th ranking restaurants) replotted with number of rewards earned on day 7 on the x-axis. Horizontal dashed
701 gray line indicates delta score of 0. LINC00473 expression in mPFC abolished CPP behavior in most

preferred restaurants only in females and only in the time but not entry domain, replicated in both cohorts. Error bars represent ±1 SEM.

Supplementary Fig. 4 | Basic Restaurant Row laps and earnings metrics across testing. a Overall sex difference comparisons between males and females (collapsing across GFP and LINC00473 virus treatment within each sex). Average number of laps run in the correct direction, total rewards earned, ratio of earns / laps, and standard deviation of earns among flavors. **b** Data from (a) split by GFP and LINC groups. **c** Data from main Fig. 3d split by sex and virus groups depicting change in rewards earned in each restaurant comparing two days at each color-coded transition point. Delta scores calculated by subtracting the following: i, day 8-7 (yellow); ii, day 13-12 (orange); iii, day 18-17 (red); iv, day 45-18 (purple). Shaded area and error bars represent ±1 SEM.

Supplementary Fig. 5 | Restaurant Row choice metrics split by flavor ranking across testing. a Average number of enter decisions made in the offer zone split by sex and virus treatment groups as well as the 4th and 1st ranking restaurant. **b** Number of skip decisions made in the offer zone. **c** Offer zone reaction time before making an enter or skip decision calculated from offer zone entry (tone onset) to either a right turn into the wait zone (enter) or a left turn into the hallway (skip). **d** Number of quit decisions made in the wait zone during a countdown. **e** The probability of quitting in the wait zone given the animal entered. This normalizes the likelihood of quitting to enter frequency. **f** Wait zone latency to quit reaction time from countdown onset (wait zone entry) until mice leave the wait zone prematurely. Shaded area represents ±1 SEM.

Supplementary Fig. 6 | Longitudinal economic analysis of decision policy optimization for food security vs. subjective value. Analysis underlying data from main Fig. 4g-i derived from Durand-de Cuttoli et al 2023 *Biological Psychiatry* [33]. **a** Computer Restaurant Row simulation of total number of pellets earned. The ideal threshold required to obtain the theoretical maximum number of pellets when ignoring flavor preferences was empirically determined to be 10 s. **b** Relative ratio of earns among restaurants for an example mouse on day 7 between the flavor rankings (i.e., this mouse had a 3.7 : 2.1 : 1.4 : 1 ratio of

earns across flavors capturing a summary of idealized relative subjective value for this mouse when all offers were 1 s only). **c** Two intersecting planes of decision policies that yield varying amounts of theoretical value either for maximal food intake (as determined by computer simulations, brown plane) or subjective value (as determined by multiplying day 7 preference ratios on a mouse-by-mouse basis, pink plane) when in a reward-scarce environment (1 to 30 s offers). Here, only two decision policy dimensions (least preferred and most preferred restaurants) of the four dimensions (all four ranked restaurants) are displayed. Both planes are normalized to each's min and max values for the purpose of plotting both in the same space while preserving the threshold coordinate locations that achieve either theoretical maximum (brown [location always fixed at threshold coordinates of 10 s] or pink beacons [location of discovered threshold coordinates that vary from mouse-to-mouse]). Actual observed daily decision policies represented by the cyan beacon wander throughout this space from day 18 to 45 in a reward-scarce environment. Trajectories projected to the floor of this display trace out individual mouse decision policy paths. Example coordinates of brown, pink, and cyan beacons illustrated as dots on the x and y axes. Euclidean distance from cyan coordinates to either brown or pink coordinates were calculated (question mark symbols). **d** Euclidean distances from observed decision policies in the offer zone (left) or wait zone (right) to either food (brown) or preference (magenta) theoretical maximum across testing in a reward-scarce environment split by GFP (top) and LINC (bottom) groups and sex. Shaded area represents ±1 SEM.

Supplementary Fig. 7 | Sensitivity to sunk costs analysis during the 1-15 s testing epoch. Mice do not display sensitivity to sunk costs during days 13-17 in a relatively reward rich environment compared to days 18+ (when offers range 1-30 s, as in main Fig. 5). **a-c** Sunk cost analysis of staying behavior in the wait zone, demonstrated using all 40 mice. (f) The likelihood of staying in the wait zone and earning a reward (e.g., not quit) is plotted as a function of time left in the countdown along the x-axis and time already spent waiting orthogonally in color. Note the black 0 s time spent curve represents animals having just entered the wait zone from the offer zone. Inset vertical dashed gray line illustrates an example analysis point comparing three sunk cost conditions originating from different starting offers but matched at 10 s left. Data from (a) dimensioned reduced in (b) collapsing across time left, highlighting the grand mean of each time spent sunk cost condition (color and x-axis). Difference between curves in (b) are plotted in (c) in order

758 to summarize the envelope of the overall effect of time already spent on escalating the commitment of
759 staying in the wait zone. Horizontal dashed line represents delta score of 0. **d** Data in (c) split by sex and
760 virus treatment groups depicting no effect of time spent during the countdown in the wait zone on changing
761 the probability of quitting vs. staying to earn a reward. **e** To compare to time spent waiting in the wait zone,
762 data here depict a different type of time spent on the task: time spent in the offer zone prior to accepting an
763 offer and entering the wait zone does not influence the probability of quitting vs. staying to earn a reward
764 once in the wait zone. These data are from the 1-30 s reward-scarce epoch (days 18-45) to demonstrate
765 the unique value of time spent waiting in the wait zone uniquely conferring sunk cost sensitivity. Error bars
766 represent ±1 SEM.
767
768 **Supplementary Fig. 8 | Full set of task information manipulations on Restaurant Row. A** After day
769 45, mice were challenged with special probe days on three different task informational manipulations each
770 for 2 days. Manipulations took the form of silencing and withholding tone presentation either in the offer
771 zone, wait zone, or both: (i) silent offer zone but audible wait zone [days 46-47], (ii) audible offer zone but
772 silent wait zone [days 48-49], and (iii) silent offer zone and silent wait zone [days 50-51]. **b** Offer zone
773 choice probability to enter as a function of offer cost split by restaurants ranked from least (4th) to most (1st)
774 preferred separating sex and virus treatment groups (rows) across the 4 different task information
775 conditions (columns). **c** Data in (b) collapsed across all four restaurants showing summary enter
776 probabilities as a function of offer cost. Note that enter probabilities are largely unaffected when the offer
777 zone tones are audible comparing baseline (black, regular task) to silent wait zone (blue) conditions,
778 however, as intended, offer zone choice probabilities change into a flat horizontal line in both the silent offer
779 zone (green) and silent task (gray) conditions, as animals do not have any tone information in the offer zone
780 during these conditions. **d** Wait zone thresholds plotted as a relative fold change comparing each condition
781 to the regular task audible baseline separated across the three information manipulations (silent offer zone,
782 left, green; silent wait zone, middle, blue; silent task, right, gray) split by restaurants ranked from least (4th)
783 to most (1st) preferred, sex, and virus treatment groups. Note the difference in patterns in changes in wait
784 zone thresholds across restaurants between sex/virus groups and across task information manipulation
785 conditions. Shaded area and error bars represent ±1 SEM.

786 **Methods**

787 *Subjects:* Adult male and female C57BL/6J mice (Jackson, 10wks, n=40) were used. Mice
788 were individually housed and maintained on a 12-hr light/dark cycle with ad libitum water, only
789 food-restricted during Restaurant Row testing, conducted during their light phase. Experiments
790 were approved by the Mount Sinai Institutional Animal Care and Use Committee (IACUC; protocol
791 number LA12-00051) and adhered to the National Institutes of Health (NIH) guidelines.

792

793 *Viral constructs:* To achieve long-term neuronal expression of LINC00473, it was
794 subcloned into an AAV plasmid with human synapsin promoter (hSyn) driving gene expression.
795 LINC00473 transcript variant 1, (NR_026860.1 /AK289375) of 1821bp length was subcloned from
796 p1005+ HSV vector (PMID: 32304628) into pAAV-hSyn-eGFP-hSny plasmid (PMID: 36449610)
797 using blunt ligation into a PMEI and EcoRV restriction sites following the second hSyn promoter.
798 The orientation and sequence were validated using Sanger sequencing. Empty plasmid
799 expressing eGFP only was used as control. These vectors were used to generate AAV serotype
800 2 at the University of Maryland virus vector core. Viral vector placement and expression were
801 confirmed in vivo by a GFP fluorescent flashlight and qPCR.

802

803 *RNA extraction, RT, and qPCR:* Total RNA was isolated and purified with RNeasy Micro
804 Kit (Qiagen), using QIAzol as a lysis reagent, including DNase treatment. All samples were tested
805 for concentration and purity using a NanoDrop (Thermo Fisher). RNA amount was normalized
806 across samples (400ng), and cDNA was created using iScript (Bio-Rad). Real-time PCR reactions
807 were run in triplicate using PowerUp SYBR Master Mix (Applied Biosystems) in a QuantStudio 7
808 (Thermo Fisher) qPCR machine. Primer sequences: LINC00473: forward:
809 GCATACTTTGGCGGACCTTTT, reverse TGTGCCTCCCTGTGAATTCTC; HPRT1 forward:
810 GCAGTACAGCCCCAAAATGG, reverse: GGTCCTTTTCACCAGCAAGCT; GFP forward:

811 CATGCCCGAAGGCTACGT, reverse CGATGCCCTTCAGCTCGAT. Raw Ct values are
812 presented and not normalized amounts, as LINC00473 is not endogenously expressed in mice.
813
814 *Virus surgery:* Mice were anesthetized by intraperitoneal injection with a mixture of
815 Ketamine HCl (100 mg/kg) and Xylazine (10 mg/kg) and positioned on a stereotaxic instrument
816 (David Kopf Instruments). In the medial prefrontal cortex (mPFC, from bregma with an angle of
817 15 degrees: AP +1.8 mm; ML ±0.75 mm; DV −2.7 mm), 0.7 µL of virus (AAV2-hSyn-GFP or AAV2-
818 hSyn-LINC00473-GFP) was bilaterally infused using 33-Gauge Hamilton needles over 5 min at a
819 rate of 0.1 µL/min, and the needle was left in place for 10-15 min after the injection before
820 retraction. Mice were allotted 2 weeks to recover before beginning food restriction across 3-4 days
821 in preparation for testing on Restaurant Row. An initial virus validation cohort (independent cohort
822 of n=10 mice) was injected with GFP or LINC00473 viruses bilaterally in mPFC at a titer of $1x10^{12}$
823 at. These animals were tested on Restaurant Row for only 1 week (offers remained at 1 s only,
824 first epoch, green) after which they were sacrificed for PCR validation on tissue punches obtained
825 from mPFC. Behavioral data from these animals on the conditioned-place preference probe (days
826 0 and 8) appear in Supplementary Fig. 3. A second replication cohort (n=40 mice) was injected
827 with GFP or LINC00473 viruses bilaterally in mPFC at a titer of $5x10^{12}$ and served as the primary
828 cohort of animals for the main figures that underwent the full 45-day longitudinal behavioral
829 testing.
830
831 *Neuroeconomic Task:* Following surgery, we characterized mice longitudinally in
832 Restaurant Row [5]. On this task, mice had a limited time period each day to forage for food by
833 navigating a maze with four uniquely flavored (chocolate, banana, grape, and plain) and
834 contextualized (horizontal stripes, dots, triangles, vertical stripes) feeding sites, or “restaurants”
835 (Fig. 1b). Animals were allotted 30 min to forage for their primary source of food for the day.
836 Rewards used on this task were obtained from BioServe (20 mg pellets #F007120). These pellets

are full nutrition and not sucrose-only pellets that only differed in flavoring but not nutritional profile (3.6 kcal/gm calories, 59.1% carbohydrate, 18.7% protein, 6.5% ash, 5.6% fat, 4.7% fiber). Choices on this task were interdependent across trials and across days. This makes the task economic in nature, requiring animals to budget their limited time effectively in a self-paced manner in order to earn a sufficient amount of food in a closed-economy system. The cost of earning a reward took place in the form of a delay animals would have to wait cued by the pitch of a tone that sounded upon entry into each restaurant. Each restaurant had a separate offer zone (OZ) and wait zone (WZ). Upon entry into the OZ, a tone (500 ms) sounded whose pitch indicated how long of a delay mice would have to wait in a cued countdown should they enter the WZ. Mice could decide to skip an offer presented in the OZ and proceed down the hallway to the next restaurant. In the OZ, tones repeated every second held at the same pitch to repeatedly cue the offer of the current trial until mice either made a skip or enter decision. If mice decide instead to enter the WZ, this triggered a countdown with descending tone pitch stepping every second until mice either waited out the full delay and earned a food pellet or quit prematurely during the countdown. If mice made a skip or quit decision, the tone terminated, the offer was rescinded, and mice must proceed forward to the next restaurant. Mice quickly learned to only travel in one direction as animals must encounter offers serially navigating the maze in a counterclockwise direction (i.e., nothing happens if mice traverse in the wrong direction other than wasting time). Mice were tested across 45 consecutive days for the main experiment where strategies developed longitudinally as animals learned the structure of the task and the changing economic landscape.

During the first week of testing (block 1, green epoch), all trials consisted of 1 s offers only. 1 s offers were indicated by tones played at the 4,000 Hz pitch. A special probe session was inserted into this timeline immediately before (day 0) and after (day 8) the first week of testing during which mice essentially were allowed to roam the empty maze arena freely without any task components (no tones, no rewards) to examine conditioned place preference behaviors learned

through the natural experience of the first week of the task itself. The remainder of the experimental timeline continued thereafter. During the next 5 days of testing (block 2, yellow epoch), offers ranged from 1 to 5 s (4,000 Hz to 5,548 Hz in 387 Hz steps) randomly selected from a uniform distribution. For instance, if a 4 s offer was selected on a given trial, the tone presented in the OZ would be 5,161 Hz for 500 ms, and this would repeat every second indefinitely until a skip or enter decision was made. If the WZ was entered, using this example trial, this 5,161 Hz tone would step down by 387 Hz every second descending in pitch until earning (with the final tone of 4,000 Hz) or quitting prematurely. Block 3 (5 days, orange epoch) consisted of a 1 to 15 s (4,000–9,418 Hz) range. The fourth and final block (red epoch) consisted of offers ranging from 1 to 30 s (4,000–15,223 Hz) and continued for the remainder of the experiment. This block-wise protocol allowed us to examine how mice initially shaped their behavior as they learned the basic structure of the task as well as how they adjusted their foraging strategies across long timescales (days, weeks, and months) as they transitioned from reward-rich to reward-scarce environments in a stepwise manner. That is, blocks 1-3 are relatively reward rich as costs are generally low delays and rewards are easier to earn compared to block 4 which is relatively reward scarce as there are far more expensive reward offers distributed in the environment for which animals must learn to forage efficiently. The rewards used in this task only differ in flavor for which animals have subjective differences in preferences quantified below. All flavor options become increasingly scarce, equally across the longitudinal paradigm.

Rewards were delivered using a custom-built 3D-printed automated pellet dispenser that was triggered by a computer running the task programmed in ANY-Maze (Stoelting), run under dim lighting. The task was run by video-tracking animal position in real-time where all choice contingencies are determined by the centroid of the animal's body crossing territories in the maze in combination with being required to run in a counterclockwise direction. The key zones in the maze include each restaurant's separate OZ and WZ as well as the hallways in between

restaurants (thus, 12 total main zones). 6 key behavioral epochs make up all possible, mutually exclusive behaviors animals could be engaged in while spending their limited time budget. 1) **Enter time**: defined from OZ entry in the correct heading direction (counterclockwise around the maze) triggering tone onset until the animal physically enters right into the WZ triggering tone countdown. 2) **Skip time**: defined from OZ entry in the correct heading direction triggering tone onset until the animal physically exits left into the hallway. 3) **Quit time**: defined from WZ entry and tone countdown onset until the animal physically exits the WZ prematurely before the countdown completes, rescinding the offer and terminating the countdown. 4) **Earn time**: defined from WZ entry and tone countdown onset until the countdown completes and a pellet is delivered. 5) **Consumption time**: defined from reward delivery onset until the animal physically leaves the reward site and exits the WZ. 6) **Travel time**: defined from previous trial termination (either from a skip, quit, or consumption event as defined above) and hallway entry until the next trial begins, triggered by OZ entry into the next restaurant.

Body weight was measured twice daily, immediately before and after testing on the Restaurant Row task.

Data analysis: In addition to simple behavioral metrics like rewards earned, laps run, reaction times as described above, a key neuroeconomic behavioral metric is decision thresholds. This metric approximates indifference points in choices made either in the OZ or WZ as a function of cost and flavor. We measured the inflection point of fitting heaviside step regressions to enter versus skip choices in the OZ or earn versus quit choices in the WZ as a function of cued offer cost in each restaurant. Thresholds determined this way were used for several subsequent analyses, including calculating reward value. The value of an offer can be calculated by subtracting a trial's offer from one's WZ threshold as this reflects the relative cost normalized to each animals' willingness to wait and earn a reward (i.e., offer value <0 indicate offers typically

915 not earned and thus should be skipped in the OZ or quit in the WZ as determined by each animal's
916 subjective flavor-specific decision policy which remained relatively stable across block 4 of
917 testing). Similarly, when quitting in the WZ, the value left at the moment of quitting can be
918 calculated by subtracting the time remaining in that trial's countdown from the WZ threshold (i.e.,
919 value left <0 indicates an amount of time left that is not worth waiting for and should have been
920 quit whereas value left >0 would have been more advantageous to finish waiting at that point
921 instead of quitting). The amount of time spent remaining in the countdown at the moment of
922 quitting relative to what the starting offer was and how much time was spent also served as the
923 basis of our analysis of sensitivity to sunk costs, as previously published in mice, rats, and humas
924 whereby time spent waiting can decrease the probability of quitting independent of time left in the
925 countdown, see Sweis et al *Science* for the development of this analysis [44, 46, 48, 49, 53].
926 Thresholds as well as economic choice history serve as the basis and criteria used in regret-
927 related analysis whereby distinct violation vs. non-violation sequences are compared head-to-
928 head in order to quantify the effects of mistake history on influencing choice behavior on the next
929 trial. See Steiner and Redish 2014 *Nature Neuroscience* [47], Sweis et al 2018 *PloS Biology* [5],
930 and Durand-de Cuttoli 2022 *Science Advances* [48] for the development of these analyses.
931 Thresholds were also used for an analysis we recently developed to capture how mice develop
932 strategies that optimize food yield while also maximizing subjective value, see Durand-de Cuttoli
933 et al 2023 *Biological Psychiatry* [33] for the development of this analysis.
934
935 Data were processed in Matlab with statistical analyses in JMP Pro 17. All data are
936 expressed as mean ± 1 standard error. Statistical significance was assessed using student's t
937 tests, sign tests, and one-way, two-way, three-way, and repeated measures ANOVAs. No data
938 were excluded as outliers.

939 **References**

940 1. Stone, C., J.B. Mattingley, and D. Rangelov, *On second thoughts: changes of mind in*
941 *decision-making.* Trends Cogn Sci, 2022. **26**(5): p. 419-431.
942 2. Liu, X., et al., *Common and distinct networks underlying reward valence and processing*
943 *stages: a meta-analysis of functional neuroimaging studies.* Neurosci Biobehav Rev,
944 2011. **35**(5): p. 1219-36.
945 3. Redish, A.D., *The mind within the brain: How we make decisions and how those decisions*
946 *go wrong.* 2013: Oxford University Press.
947 4. McGuire, J.T. and J.W. Kable, *Medial prefrontal cortical activity reflects dynamic re-*
948 *evaluation during voluntary persistence.* Nat Neurosci, 2015. **18**(5): p. 760-6.
949 5. Sweis, B.M., M.J. Thomas, and A.D. Redish, *Mice learn to avoid regret.* PLoS Biol, 2018.
950 **16**(6): p. e2005853.
951 6. Kirkebøen, G., E. Vasaasen, and K. Halvor Teigen, *Revisions and Regret: The Cost of*
952 *Changing your Mind.* Journal of Behavioral Decision Making, 2011. **26**(1): p. 1-12.
953 7. Brenner, C., *The mind in conflict*. 1982, New York: International Universities Press. 266 p.
954 8. Baumeister, R.F., K.D. Vohs, and D.M. Tice, *The Strength Model of Self-Control.* Current
955 Directions in Psychological Science, 2016. **16**(6): p. 351-355.
956 9. American Psychiatric Association. and American Psychiatric Association. DSM-5 Task
957 Force., *Diagnostic and statistical manual of mental disorders : DSM-5*. 5th ed. 2013,
958 Washington, D.C.: American Psychiatric Association. xliv, 947 p.
959 10. Mezo, P.G. and R.M. Baker, *The moderating effects of stress and rumination on*
960 *depressive symptoms in women and men.* Stress Health, 2012. **28**(4): p. 333-9.
961 11. Seedat, S., et al., *Cross-National Associations Between Gender and Mental Disorders in*
962 *the World Health Organization World Mental Health Surveys.* Archives of General
963 Psychiatry, 2009. **66**(7).

964 12. Ferrari, A.J., et al., *Burden of depressive disorders by country, sex, age, and year: findings*
965 *from the global burden of disease study 2010.* PLoS Med, 2013. **10**(11): p. e1001547.
966 13. Marcus, S.M., et al., *Sex differences in depression symptoms in treatment-seeking adults:*
967 *confirmatory analyses from the Sequenced Treatment Alternatives to Relieve Depression*
968 *study.* Compr Psychiatry, 2008. **49**(3): p. 238-46.
969 14. Silverstein, B., *Gender differences in the prevalence of somatic versus pure depression:*
970 *a replication.* Am J Psychiatry, 2002. **159**(6): p. 1051-2.
971 15. Martin, L.A., H.W. Neighbors, and D.M. Griffith, *The experience of symptoms of*
972 *depression in men vs women: analysis of the National Comorbidity Survey Replication.*
973 JAMA Psychiatry, 2013. **70**(10): p. 1100-6.
974 16. Eid, R.S., A.R. Gobinath, and L.A.M. Galea, *Sex differences in depression: Insights from*
975 *clinical and preclinical studies.* Prog Neurobiol, 2019. **176**: p. 86-102.
976 17. Akil, H., et al., *Treatment resistant depression: A multi-scale, systems biology approach.*
977 Neurosci Biobehav Rev, 2018. **84**: p. 272-288.
978 18. Ulitsky, I. and D.P. Bartel, *lincRNAs: genomics, evolution, and mechanisms.* Cell, 2013.
979 **154**(1): p. 26-46.
980 19. Issler, O., et al., *Sex-Specific Role for the Long Non-coding RNA LINC00473 in*
981 *Depression.* Neuron, 2020. **106**(6): p. 912-926 e5.
982 20. Chen, Z., et al., *cAMP/CREB-regulated LINC00473 marks LKB1-inactivated lung cancer*
983 *and mediates tumor growth.* J Clin Invest, 2016. **126**(6): p. 2267-79.
984 21. Jiang, L.Y., et al., *CREB-induced LINC00473 promotes chemoresistance to TMZ in*
985 *glioblastoma by regulating O6-methylguanine-DNA-methyltransferase expression via*
986 *CEBPalpha binding.* Neuropharmacology, 2024. **243**: p. 109790.
987 22. Ataman, B., et al., *Evolution of Osteocrin as an activity-regulated factor in the primate*
988 *brain.* Nature, 2016. **539**(7628): p. 242-247.

989 23. Pruunsild, P., et al., *Expression of the primate-specific LINC00473 RNA in mouse neurons*
990 *promotes excitability and CREB-regulated transcription.* J Biol Chem, 2023. **299**(5): p.
991 104671.
992 24. Pruunsild, P., C.P. Bengtson, and H. Bading, *Networks of Cultured iPSC-Derived Neurons*
993 *Reveal the Human Synaptic Activity-Regulated Adaptive Gene Program.* Cell Rep, 2017.
994 **18**(1): p. 122-135.
995 25. Tran, K.V., et al., *Human thermogenic adipocyte regulation by the long noncoding RNA*
996 *LINC00473.* Nat Metab, 2020. **2**(5): p. 397-412.
997 26. Glimcher, P.W. and A. Rustichini, *Neuroeconomics: the consilience of brain and decision.*
998 Science, 2004. **306**(5695): p. 447-52.
999 27. Kenning, P. and H. Plassmann, *Neuroeconomics: an overview from an economic*
1000 *perspective.* Brain Res Bull, 2005. **67**(5): p. 343-54.
1001 28. Loewenstein, G., S. Rick, and J.D. Cohen, *Neuroeconomics.* Annu Rev Psychol, 2008.
1002 **59**: p. 647-72.
1003 29. Kalenscher, T. and C.M. Pennartz, *Is a bird in the hand worth two in the future? The*
1004 *neuroeconomics of intertemporal decision-making.* Prog Neurobiol, 2008. **84**(3): p. 284-
1005 315.
1006 30. Clithero, J.A. and A. Rangel, *Informatic parcellation of the network involved in the*
1007 *computation of subjective value.* Soc Cogn Affect Neurosci, 2014. **9**(9): p. 1289-302.
1008 31. Levy, D.J. and P.W. Glimcher, *The root of all value: a neural common currency for choice.*
1009 Curr Opin Neurobiol, 2012. **22**(6): p. 1027-38.
1010 32. Louie, K. and P.W. Glimcher, *Efficient coding and the neural representation of value.* Ann
1011 N Y Acad Sci, 2012. **1251**: p. 13-32.
1012 33. Durand-de Cuttoli, R., et al., *A double-hit of social and economic stress in mice precipitates*
1013 *changes in decision-making strategies.* Biol Psychiatry, 2023.

1014 34. Resulaj, A., et al., *Changes of mind in decision-making.* Nature, 2009. **461**(7261): p. 263-
1015 6.
1016 35. Hare, T.A., C.F. Camerer, and A. Rangel, *Self-control in decision-making involves*
1017 *modulation of the vmPFC valuation system.* Science, 2009. **324**(5927): p. 646-8.
1018 36. Alagapan, S., et al., *Cingulate dynamics track depression recovery with deep brain*
1019 *stimulation.* Nature, 2023. **622**(7981): p. 130-138.
1020 37. Knutson, B., et al., *Neural responses to monetary incentives in major depression.* Biol
1021 Psychiatry, 2008. **63**(7): p. 686-92.
1022 38. Holton, E., et al., *Goal commitment is supported by vmPFC through selective attention.*
1023 Nature Human Behaviour, 2024.
1024 39. Sweis, B.M. and E.J. Nestler, *Pushing the boundaries of behavioral analysis could aid*
1025 *psychiatric drug discovery.* PLoS Biol, 2022. **20**(12): p. e3001904.
1026 40. Sweis, B.M., M.J. Thomas, and A.D. Redish, *Beyond simple tests of value: measuring*
1027 *addiction as a heterogeneous disease of computation-specific valuation processes.* Learn
1028 Mem, 2018. **25**(9): p. 501-512.
1029 41. Abram, S.V., et al., *The Web-Surf Task: A translational model of human decision-making.*
1030 Cogn Affect Behav Neurosci, 2016. **16**(1): p. 37-50.
1031 42. Maisson, D., et al., *Widespread coding of navigational variables in prefrontal cortex*
1032 biorxiv, 2022.
1033 43. McInnes, A.N., et al., *Psychometric validation and clinical correlates of an experiential*
1034 *foraging task.* BioRxiv, 2023. **2023.12.28.573439**.
1035 44. Kazinka, R., A.W. MacDonald, 3rd, and A.D. Redish, *Sensitivity to Sunk Costs Depends*
1036 *on Attention to the Delay.* Front Psychol, 2021. **12**: p. 604843.
1037 45. Abram, S.V., et al., *Neural signatures underlying deliberation in human foraging decisions.*
1038 Cogn Affect Behav Neurosci, 2019. **19**(6): p. 1492-1508.

1039 46. Sweis, B.M., et al., *Sensitivity to "sunk costs" in mice, rats, and humans.* Science, 2018.
1040 **361**(6398): p. 178-181.
1041 47. Steiner, A.P. and A.D. Redish, *Behavioral and neurophysiological correlates of regret in*
1042 *rat decision-making on a neuroeconomic task.* Nat Neurosci, 2014. **17**(7): p. 995-1002.
1043 48. Durand-de Cuttoli, R., et al., *Distinct forms of regret linked to resilience versus*
1044 *susceptibility to stress are regulated by region-specific CREB function in mice.* Science
1045 Advances, 2022. **8**(42): p. eadd5579.
1046 49. Redish, A.D., et al., *Sunk cost sensitivity during change-of-mind decisions is informed by*
1047 *both the spent and remaining costs.* Commun Biol, 2022. **5**(1): p. 1337.
1048 50. Sweis, B.M., et al., *Altering gain of the infralimbic-to-accumbens shell circuit alters*
1049 *economically dissociable decision-making algorithms.* Proc Natl Acad Sci U S A, 2018.
1050 **115**(27): p. E6347-E6355.
1051 51. Sweis, B.M., A.D. Redish, and M.J. Thomas, *Prolonged abstinence from cocaine or*
1052 *morphine disrupts separable valuations during decision conflict.* Nat Commun, 2018. **9**(1):
1053 p. 2521.
1054 52. Diehl, G. and A.D. Redish, *Differential processing of decision information in subregions of*
1055 *rodent medial prefrontal cortex.* biorxiv, 2022.
1056 53. Duin, A.A., et al., *Certainty and uncertainty of the future changes planning and sunk costs.*
1057 Behav Neurosci, 2021.
1058 54. Schmidt, B., A.A. Duin, and A.D. Redish, *Disrupting the medial prefrontal cortex alters*
1059 *hippocampal sequences during deliberative decision making.* J Neurophysiol, 2019.
1060 **121**(6): p. 1981-2000.
1061 55. Schmidt, B. and A.D. Redish, *Disrupting the medial prefrontal cortex with designer*
1062 *receptors exclusively activated by designer drug alters hippocampal sharp-wave ripples*
1063 *and their associated cognitive processes.* Hippocampus, 2021.

1064 56. Abram, S.V., A.D. Redish, and A.W. MacDonald, 3rd, *Learning From Loss After Risk:*
1065 *Dissociating Reward Pursuit and Reward Valuation in a Naturalistic Foraging Task.* Front
1066 Psychiatry, 2019. **10**: p. 359.
1067 57. Vialou, V., et al., *DeltaFosB in brain reward circuits mediates resilience to stress and*
1068 *antidepressant responses.* Nat Neurosci, 2010. **13**(6): p. 745-52.
1069 58. German, P.W. and H.L. Fields, *Rat nucleus accumbens neurons persistently encode*
1070 *locations associated with morphine reward.* J Neurophysiol, 2007. **97**(3): p. 2094-106.
1071 59. Sjulson, L., et al., *Cocaine Place Conditioning Strengthens Location-Specific*
1072 *Hippocampal Coupling to the Nucleus Accumbens.* Neuron, 2018. **98**(5): p. 926-934 e5.
1073 60. Nwakama, C.A., et al., *Diabetes alters neuroeconomically dissociable forms of mental*
1074 *accounting.* bioRxiv, 2024.
1075 61. Camille, N., et al., *The involvement of the orbitofrontal cortex in the experience of regret.*
1076 Science, 2004. **304**(5674): p. 1167-70.
1077 62. Coricelli, G., et al., *Regret and its avoidance: a neuroimaging study of choice behavior.*
1078 Nat Neurosci, 2005. **8**(9): p. 1255-62.
1079 63. Coricelli, G., R.J. Dolan, and A. Sirigu, *Brain, emotion and decision making: the*
1080 *paradigmatic example of regret.* Trends Cogn Sci, 2007. **11**(6): p. 258-65.
1081 64. Bardo, M.T. and R.A. Bevins, *Conditioned place preference: what does it add to our*
1082 *preclinical understanding of drug reward?* Psychopharmacology, 2000. **153**(1): p. 31-43.
1083 65. Tzschentke, T.M., *Measuring reward with the conditioned place preference (CPP)*
1084 *paradigm: update of the last decade.* Addict Biol, 2007. **12**(3-4): p. 227-462.
1085 66. Johnson, A. and A.D. Redish, *Neural ensembles in CA3 transiently encode paths forward*
1086 *of the animal at a decision point.* J Neurosci, 2007. **27**(45): p. 12176-89.
1087 67. Kay, K., et al., *Constant Sub-second Cycling between Representations of Possible*
1088 *Futures in the Hippocampus.* Cell, 2020. **180**(3): p. 552-567 e25.

1089 68. Huynh, T., et al., *Vicarious Trial-and-Error Is Enhanced During Deliberation in Human*
1090 *Virtual Navigation in a Translational Foraging Task.* Front Behav Neurosci, 2021. **15**: p.
1091 586159.
1092 69. Diehl, G. and A.D. Redish, *Measuring excitation-inhibition balance through spectral*
1093 *components of local field potentials.* bioRxiv, 2024.
1094 70. Kocharian, A., *Dopaminergic control of neuroeconomic decision-making.* ProQuest,
1095 University of Minnesota, 2023.
1096 71. Lind, E.B., et al., *A quadruple dissociation of reward-related behaviour in mice across*
1097 *excitatory inputs to the nucleus accumbens shell.* Commun Biol, 2023. **6**(1): p. 119.
1098 72. Barrot, M., et al., *CREB activity in the nucleus accumbens shell controls gating of*
1099 *behavioral responses to emotional stimuli.* Proc Natl Acad Sci U S A, 2002. **99**(17): p.
1100 11435-40.
1101 73. Carlezon, W.A., Jr., R.S. Duman, and E.J. Nestler, *The many faces of CREB.* Trends
1102 Neurosci, 2005. **28**(8): p. 436-45.
1103 74. Kim, J., et al., *Memory recall and modifications by activating neurons with elevated CREB.*
1104 Nat Neurosci, 2014. **17**(1): p. 65-72.
1105 75. Lonze, B.E. and D.D. Ginty, *Function and regulation of CREB family transcription factors*
1106 *in the nervous system.* Neuron, 2002. **35**(4): p. 605-23.
1107 76. McClung, C.A. and E.J. Nestler, *Regulation of gene expression and cocaine reward by*
1108 *CREB and DeltaFosB.* Nat Neurosci, 2003. **6**(11): p. 1208-15.
1109 77. Sakai, N., et al., *Inducible and brain region-specific CREB transgenic mice.* Mol
1110 Pharmacol, 2002. **61**(6): p. 1453-64.
1111 78. Lorsch, Z.S., et al., *Stress resilience is promoted by a Zfp189-driven transcriptional*
1112 *network in prefrontal cortex.* Nat Neurosci, 2019. **22**(9): p. 1413-1423.
1113 79. Durand-de Cuttoli, R., et al., *Chronic social stress induces isolated deficits in reward*
1114 *anticipation on a neuroeconomic foraging task.* biorxiv, 2022.

1115 80. Barrot, M., et al., *Regulation of anxiety and initiation of sexual behavior by CREB in the*
1116 *nucleus accumbens.* Proc Natl Acad Sci U S A, 2005. **102**(23): p. 8357-62.
1117 81. Dong, Y., et al., *CREB modulates excitability of nucleus accumbens neurons.* Nat
1118 Neurosci, 2006. **9**(4): p. 475-7.
1119 82. Zhou, J., et al., *Effects of Estrogen Treatment on Expression of Brain-Derived*
1120 *Neurotrophic Factor and cAMP Response Element-Binding Protein Expression and*
1121 *Phosphorylation in Rat Amygdaloid and Hippocampal Structures.* Neuroendocrinology,
1122 2005. **81**(5): p. 294-310.
1123 83. Sharma, K., et al., *Chronic exposure to estrogen and tamoxifen regulates synaptophysin*
1124 *and phosphorylated cAMP response element-binding (CREB) protein expression in CA1*
1125 *of ovariectomized rat hippocampus.* Brain Res, 2007. **1132**(1): p. 10-9.
1126 84. Lorsch, Z.S., et al., *Estrogen receptor alpha drives pro-resilient transcription in mouse*
1127 *models of depression.* Nat Commun, 2018. **9**(1): p. 1116.
1128 85. Shansky, R.M., et al., *Estrogen mediates sex differences in stress-induced prefrontal*
1129 *cortex dysfunction.* Mol Psychiatry, 2004. **9**(5): p. 531-8.
1130 86. Issler, O., et al., *The long noncoding RNA FEDORA is a cell type– and sex-specific*
1131 *regulator of depression.* Science Advances, 2022. **8**(48).
1132

Figure 1

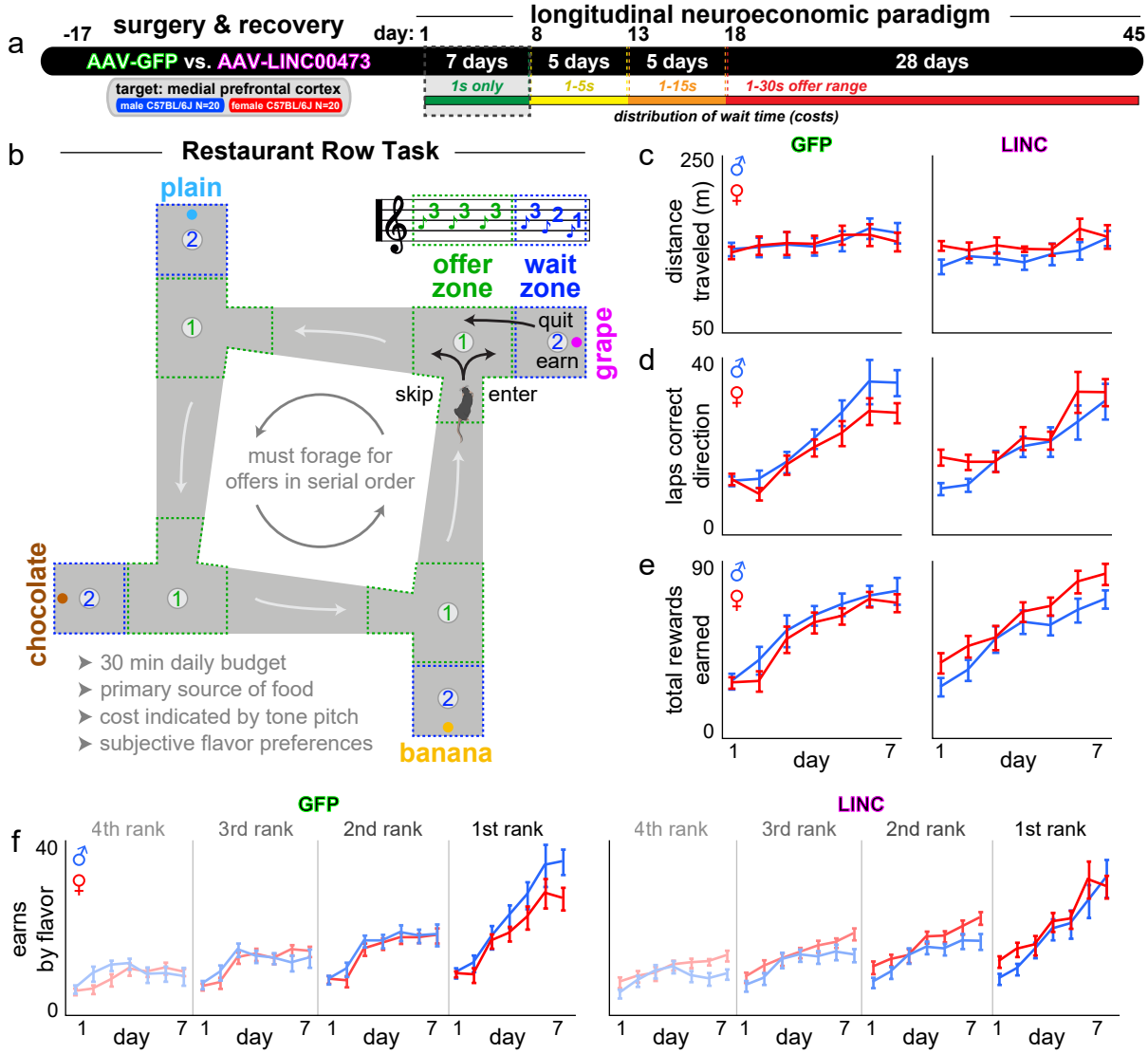
a
-17
surgery & recovery
AAV-GFP vs. AAV-LINC00473
target: medial prefrontal cortex
male C57BL/6J N=20
female C57BL/6J N=20
longitudinal neuroeconomic paradigm
day: 1
8
13
18
45
7 days
5 days
5 days
28 days
1s only
1-5s
1-15s
1-30s offer range
distribution of wait time (costs)
b
Restaurant Row Task
plain
offer zone
wait zone
quit
earn
grape
skip
enter
must forage for offers in serial order
chocolate
banana
30 min daily budget
primary source of food
cost indicated by tone pitch
subjective flavor preferences
c
GFP
LINC
distance traveled (m)
250
50
d
laps correct direction
40
0
e
total rewards earned
90
0
1
day
7
f
earns by flavor
40
0
4th rank
3rd rank
2nd rank
1st rank

Figure 2

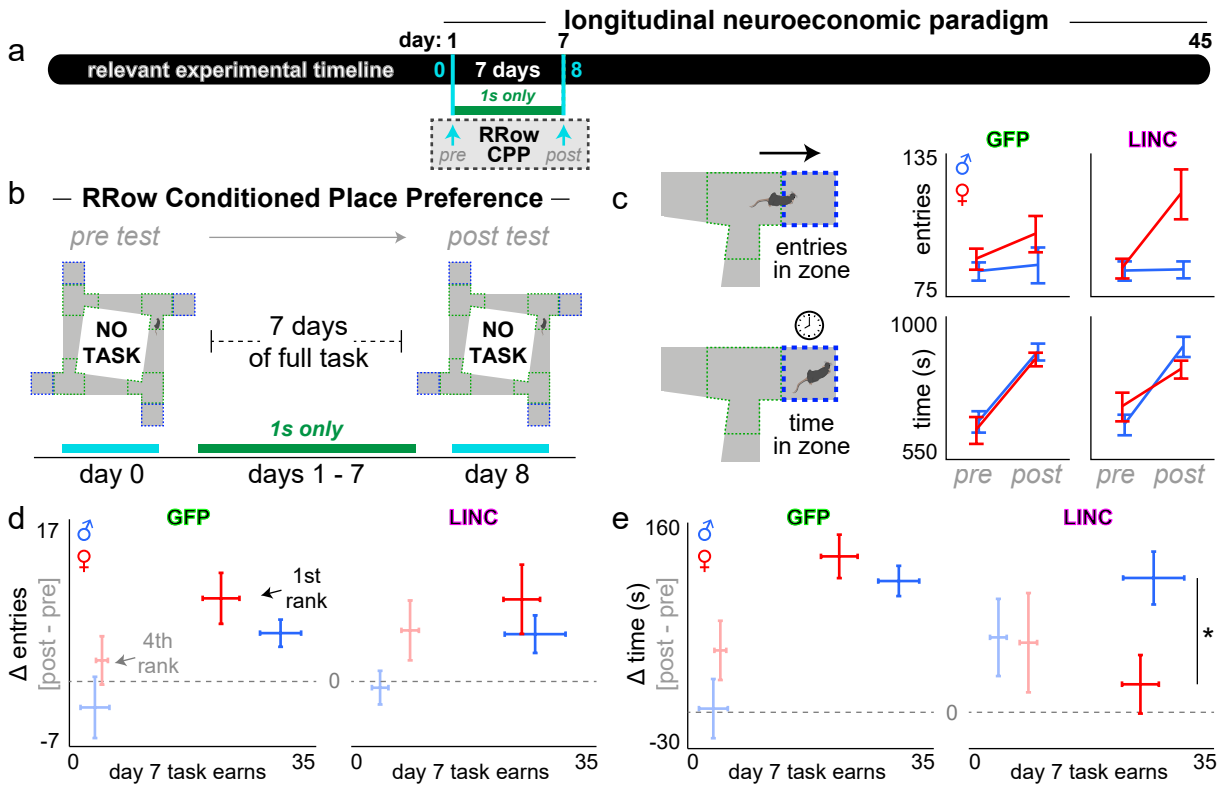
longitudinal neuroeconomic paradigm
a
day: 1
7
45
relevant experimental timeline
0
7 days
8
1s only
RRow CPP
pre
post
b
RRow Conditioned Place Preference
pre test
post test
NO TASK
7 days of full task
NO TASK
1s only
day 0
days 1 - 7
day 8
c
entries in zone
time in zone
GFP
LINC
135
entries
75
1000
time (s)
550
pre
post
pre
post
d
GFP
LINC
17
Δ entries [post - pre]
-7
1st rank
4th rank
0
0
day 7 task earns
35
0
day 7 task earns
35
e
GFP
LINC
160
Δ time (s) [post - pre]
-30
0
*
0
day 7 task earns
35
0
day 7 task earns
35

Figure 3

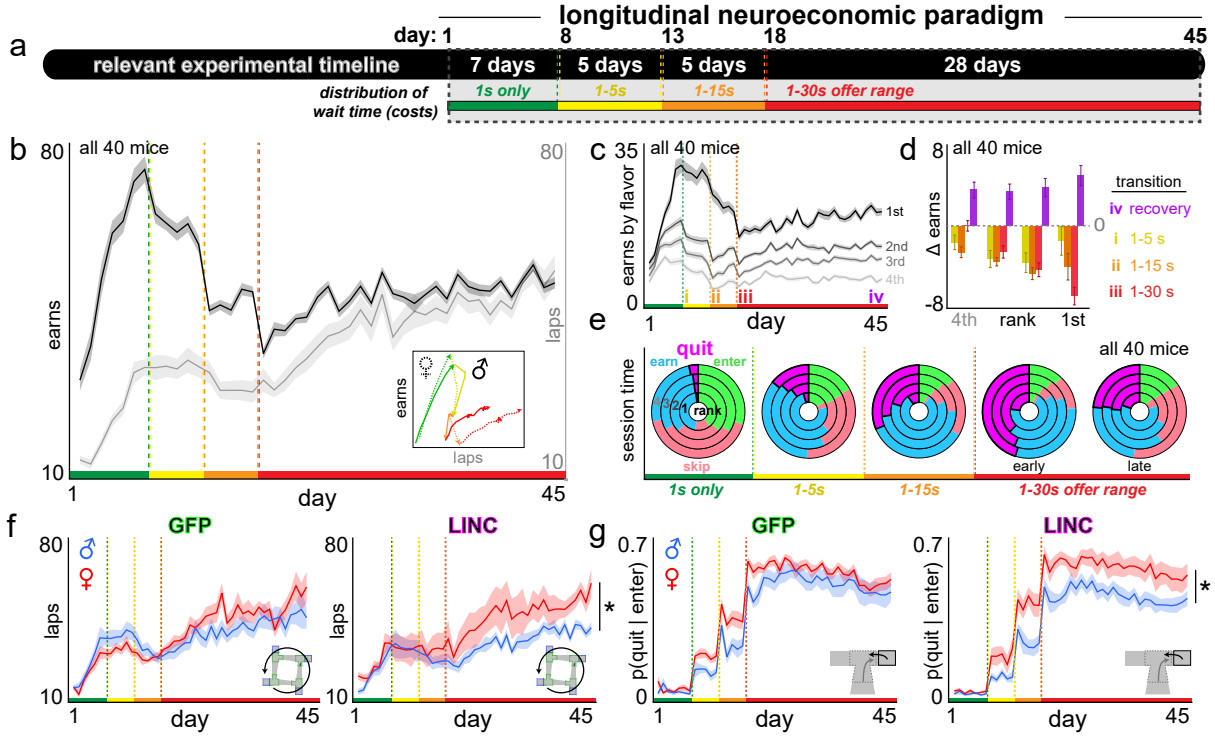
longitudinal neuroeconomic paradigm
a
day: 1
8
13
18
45
relevant experimental timeline
7 days
5 days
5 days
28 days
distribution of wait time (costs)
1s only
1-5s
1-15s
1-30s offer range
b
all 40 mice
earns
laps
day
c
all 40 mice
earns by flavor
1st
2nd
3rd
4th
i
ii
iii
iv
d
all 40 mice
Δ earns
transition
iv recovery
i 1-5 s
ii 1-15 s
iii 1-30 s
4th
rank
1st
e
quit
earn
enter
rank
skip
session time
all 40 mice
early
late
1s only
1-5s
1-15s
1-30s offer range
f
GFP
LINC
laps
day
g
GFP
LINC
p(quit | enter)
day

Figure 4

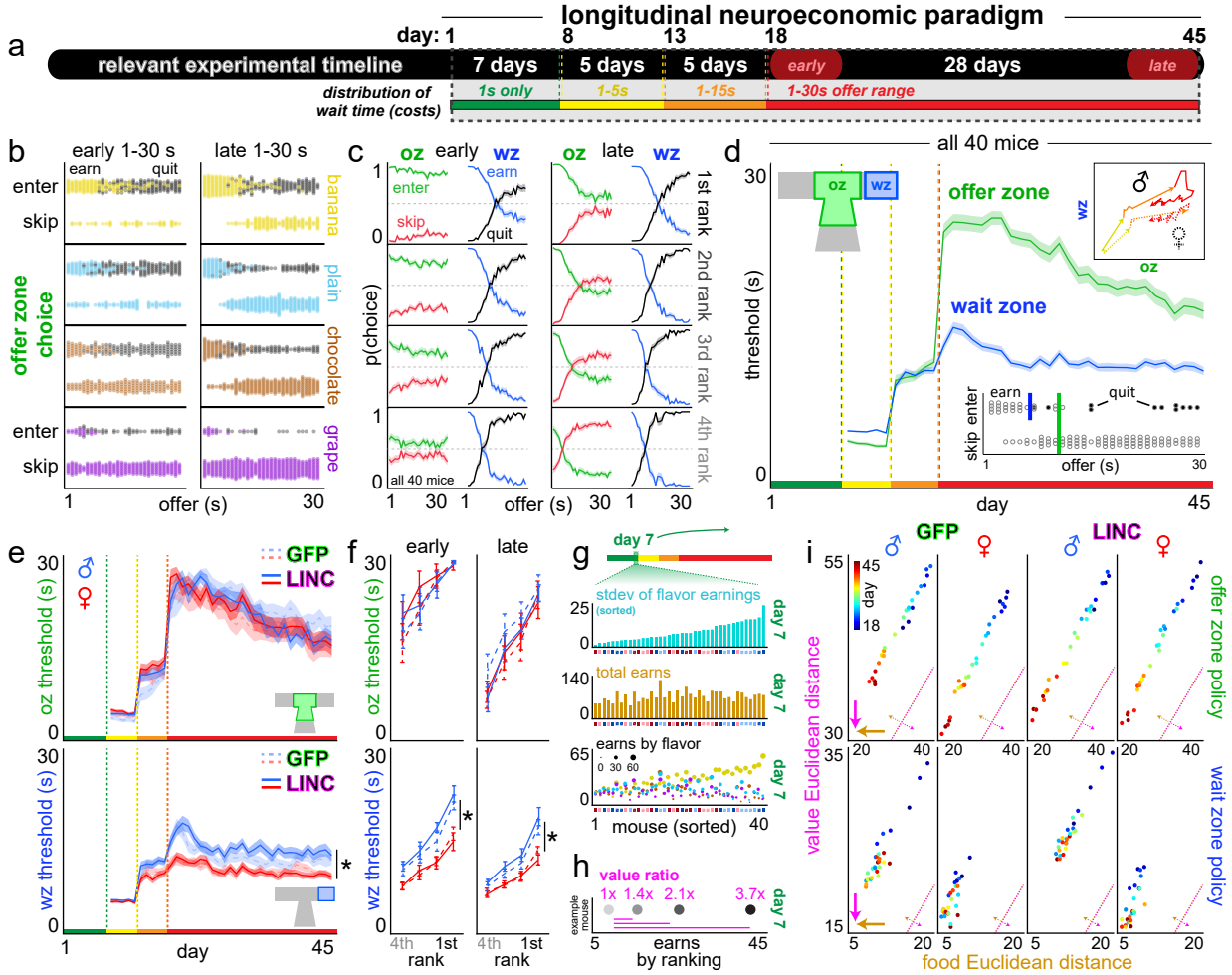
longitudinal neuroeconomic paradigm
a
day: 1
8
13
18
45
relevant experimental timeline
7 days
5 days
5 days
early
28 days
late
distribution of wait time (costs)
1s only
1-5s
1-15s
1-30s offer range
b
early 1-30 s
late 1-30 s
earn
quit
enter
skip
offer zone choice
banana
plain
chocolate
grape
offer (s)
c
oz
early
wz
late
p(choice)
1st rank
2nd rank
3rd rank
4th rank
all 40 mice
d
all 40 mice
offer zone
wait zone
threshold (s)
day
e
GFP
LINC
oz threshold (s)
wz threshold (s)
f
early
late
rank
g
day 7
stdev of flavor earnings (sorted)
total earns
earns by flavor
mouse (sorted)
h
value ratio
1x 1.4x 2.1x
3.7x
example mouse
earns by ranking
i
GFP
LINC
offer zone policy
wait zone policy
value Euclidean distance
food Euclidean distance

Figure 5

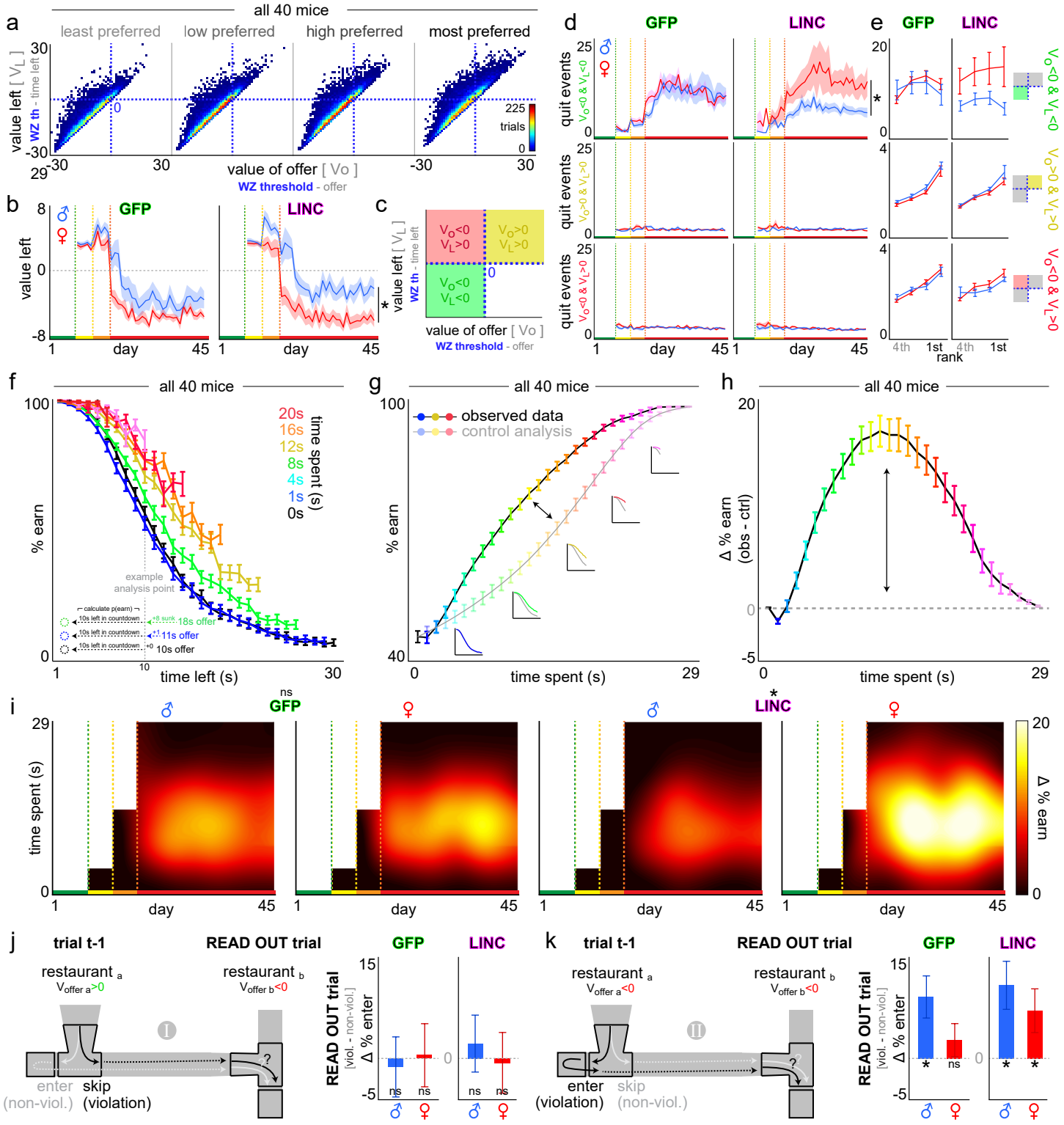
a
all 40 mice
least preferred
low preferred
high preferred
most preferred
value left [V_L]
WZ th - time left
value of offer [Vo]
WZ threshold - offer
225
trials
b
GFP
LINC
value left
day
c
V_O<0 V_L>0
V_O>0 V_L>0
V_O<0 V_L<0
d
quit events
e
rank
4th
1st
f
all 40 mice
% earn
time left (s)
time spent (s)
20s
16s
12s
8s
4s
1s
0s
example analysis point
calculate p(earn)
10s left in countdown
18s offer
11s offer
10s offer
g
observed data
control analysis
% earn
time spent (s)
h
Δ % earn (obs - ctrl)
time spent (s)
i
GFP
LINC
time spent (s)
day
Δ % earn
j
trial t-1
READ OUT trial
restaurant a
restaurant b
enter (non-viol.)
skip (violation)
READ OUT trial
Δ % enter
[viol. - non-viol.]
k
trial t-1
READ OUT trial
enter (violation)
skip (non-viol.)

Figure 6

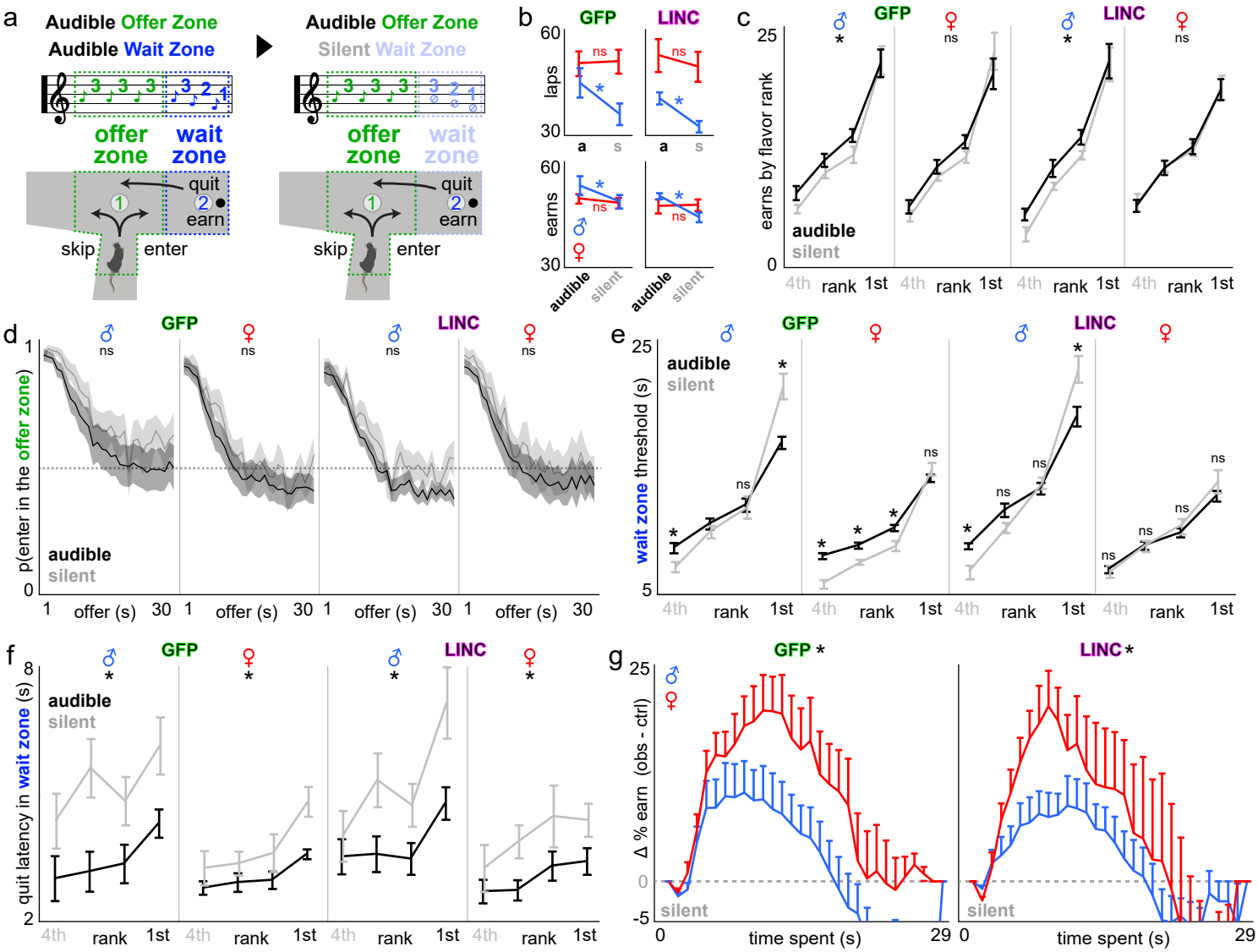
a
Audible Offer Zone
Audible Wait Zone
offer zone
wait zone
quit
earn
skip
enter
Audible Offer Zone
Silent Wait Zone
b
GFP
LINC
laps
earns
audible
silent
c
GFP
LINC
earns by flavor rank
audible
silent
4th rank 1st
d
GFP
LINC
p(enter in the offer zone)
audible
silent
offer (s)
e
GFP
LINC
wait zone threshold (s)
audible
silent
f
GFP
LINC
quit latency in wait zone (s)
audible
silent
g
GFP
LINC
Δ % earn (obs - ctrl)
silent
time spent (s)

Supplementary Figure 1

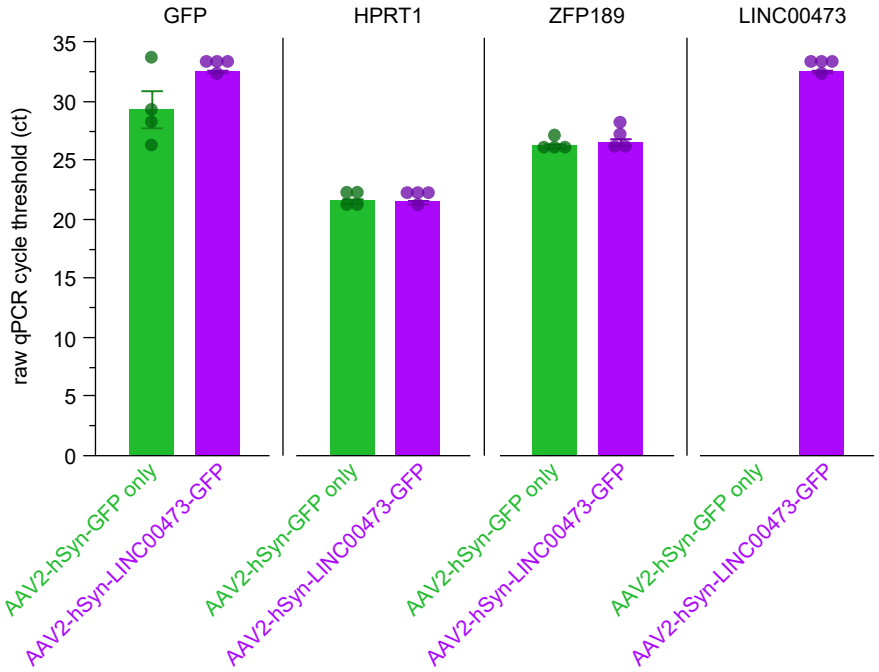

Supplementary Figure 2

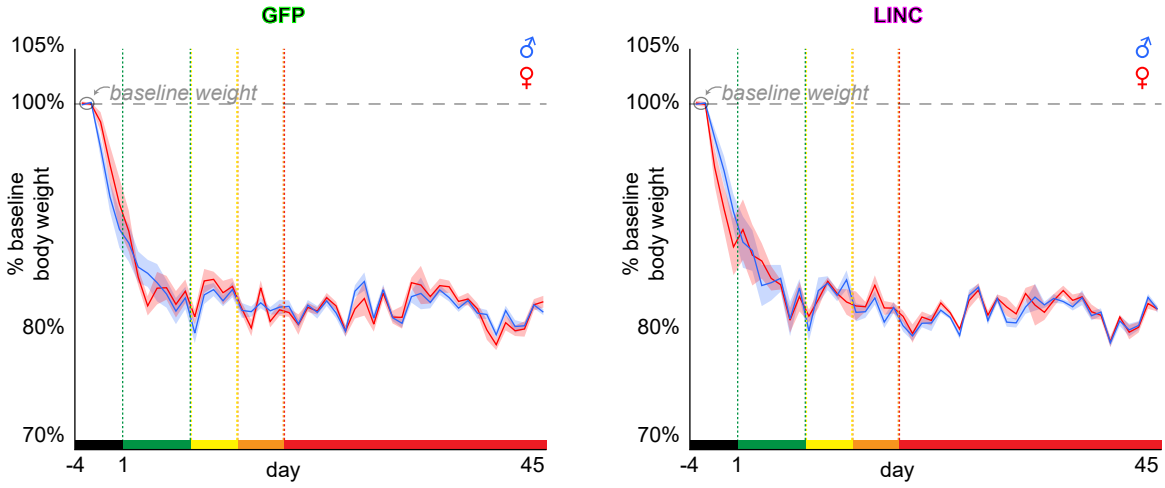

Supplementary Figure 3

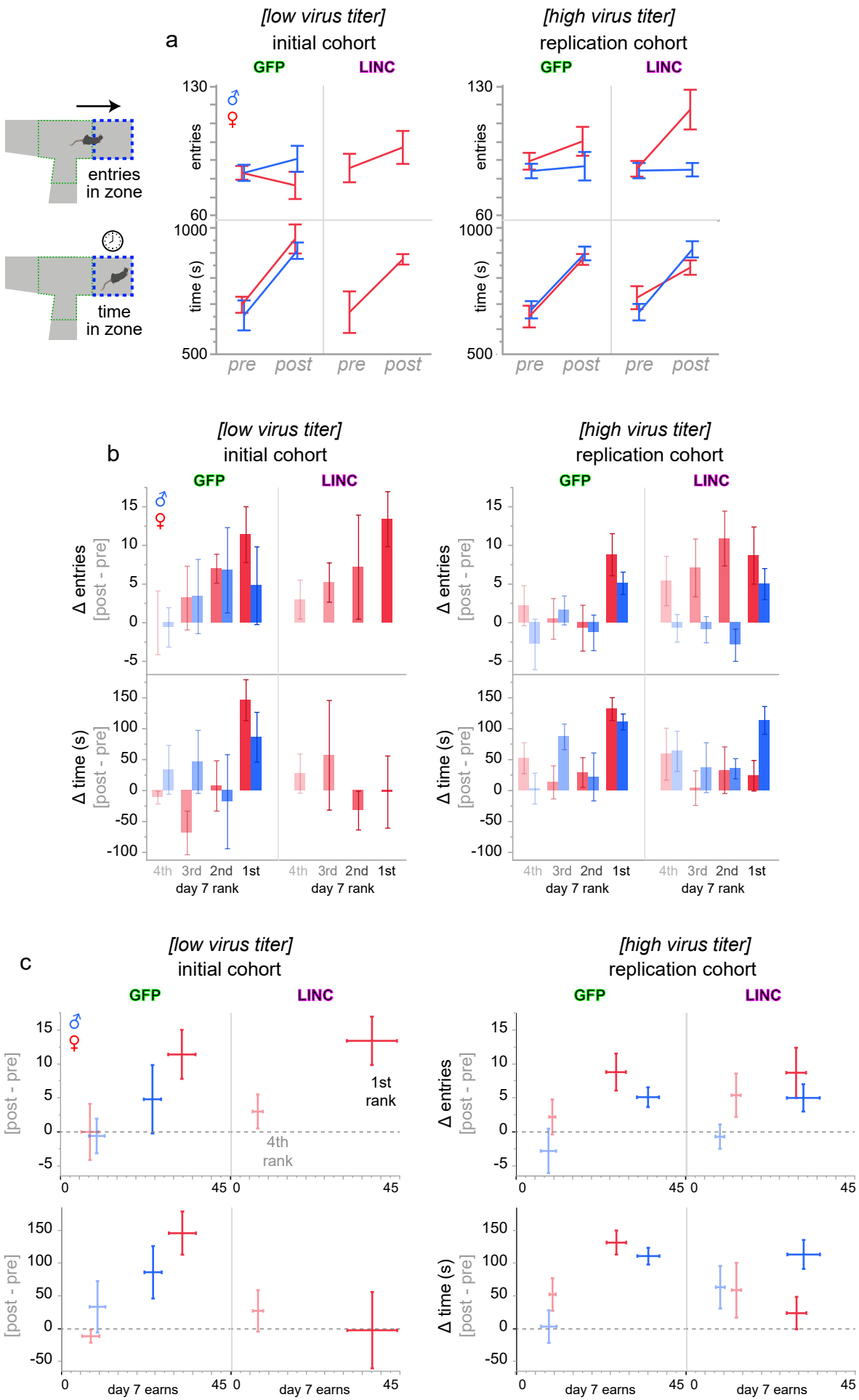

Supplementary Figure 4

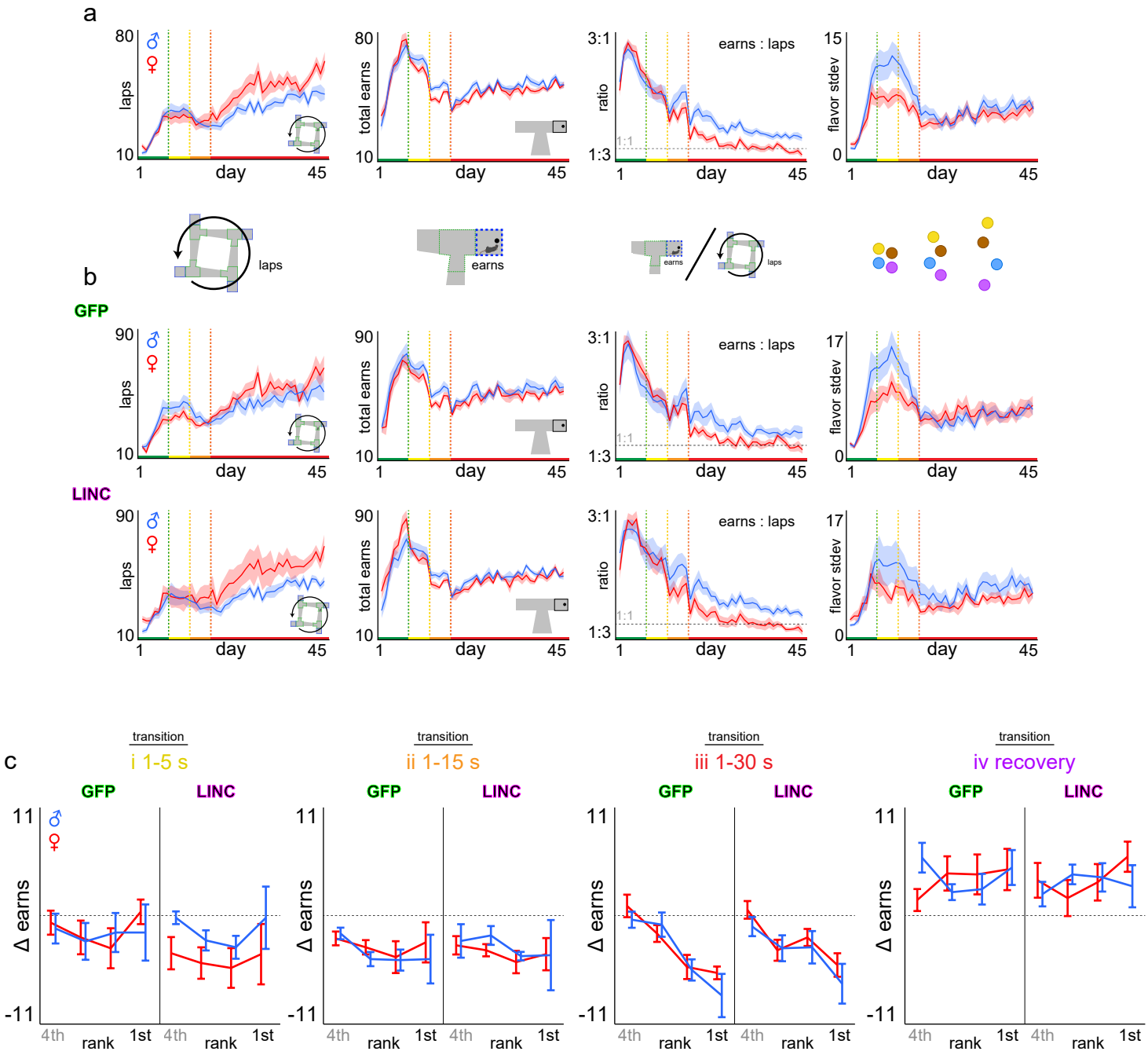

Supplementary Figure 5

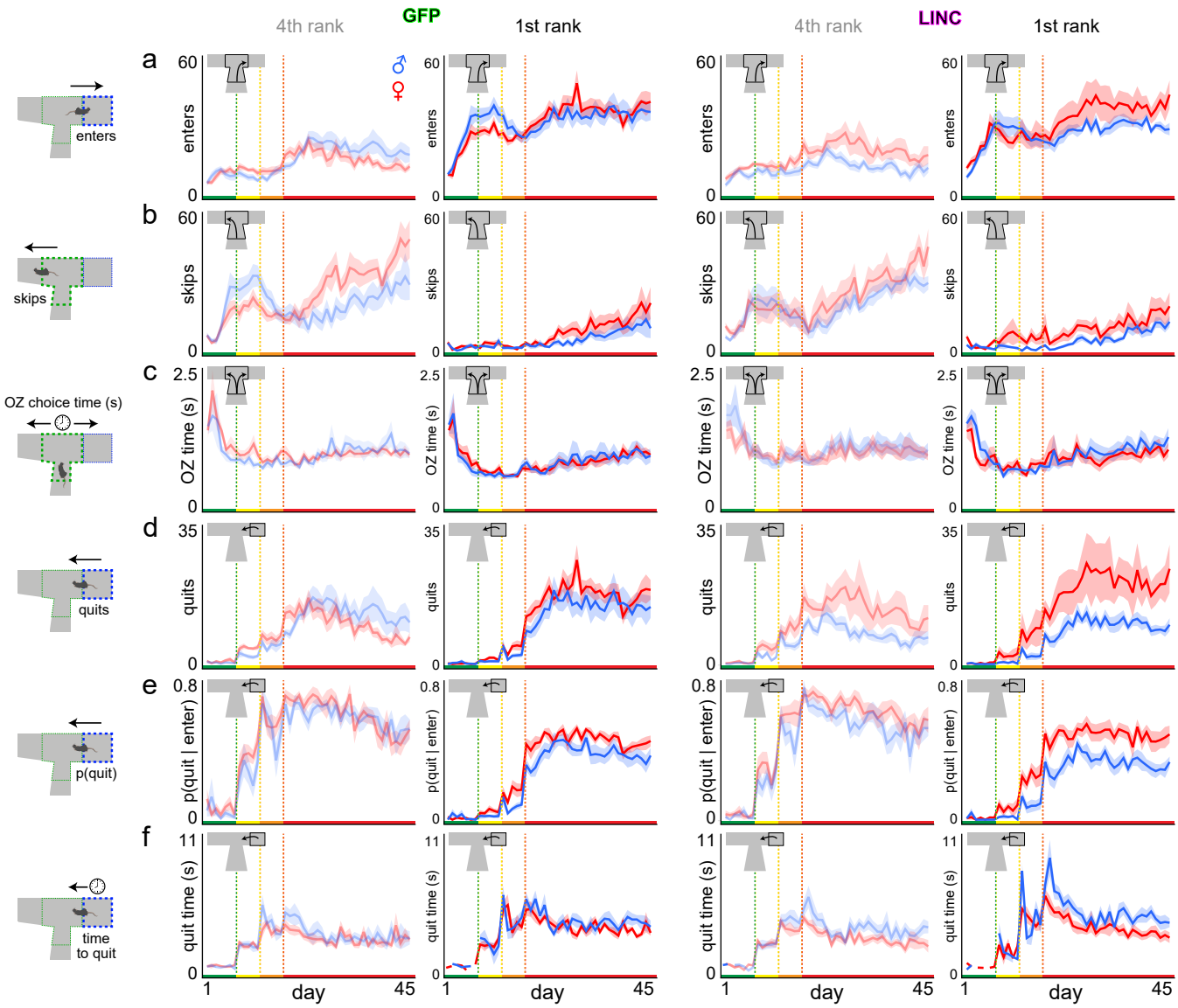

Supplementary Figure 6

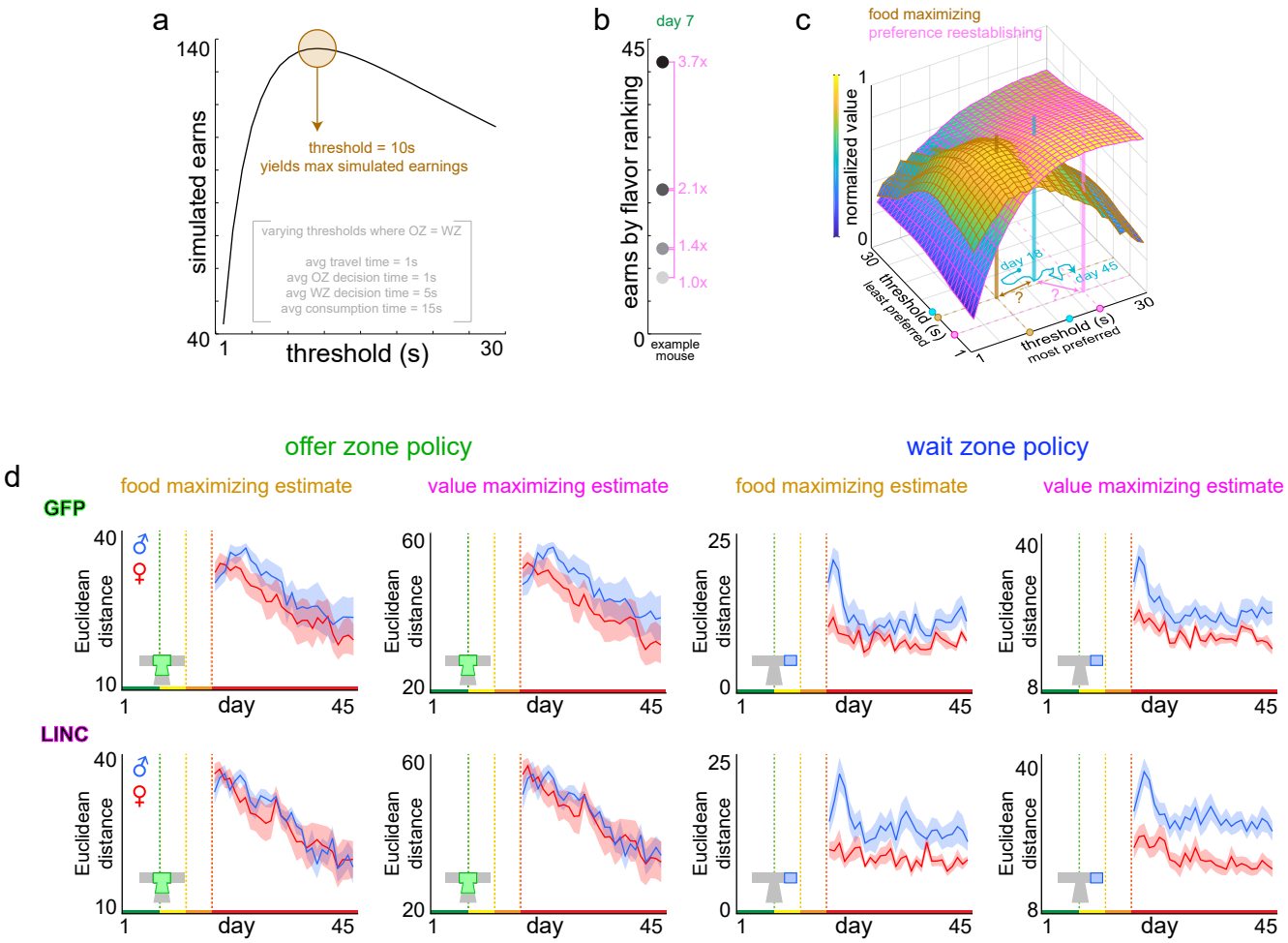

Supplementary Fig. 7

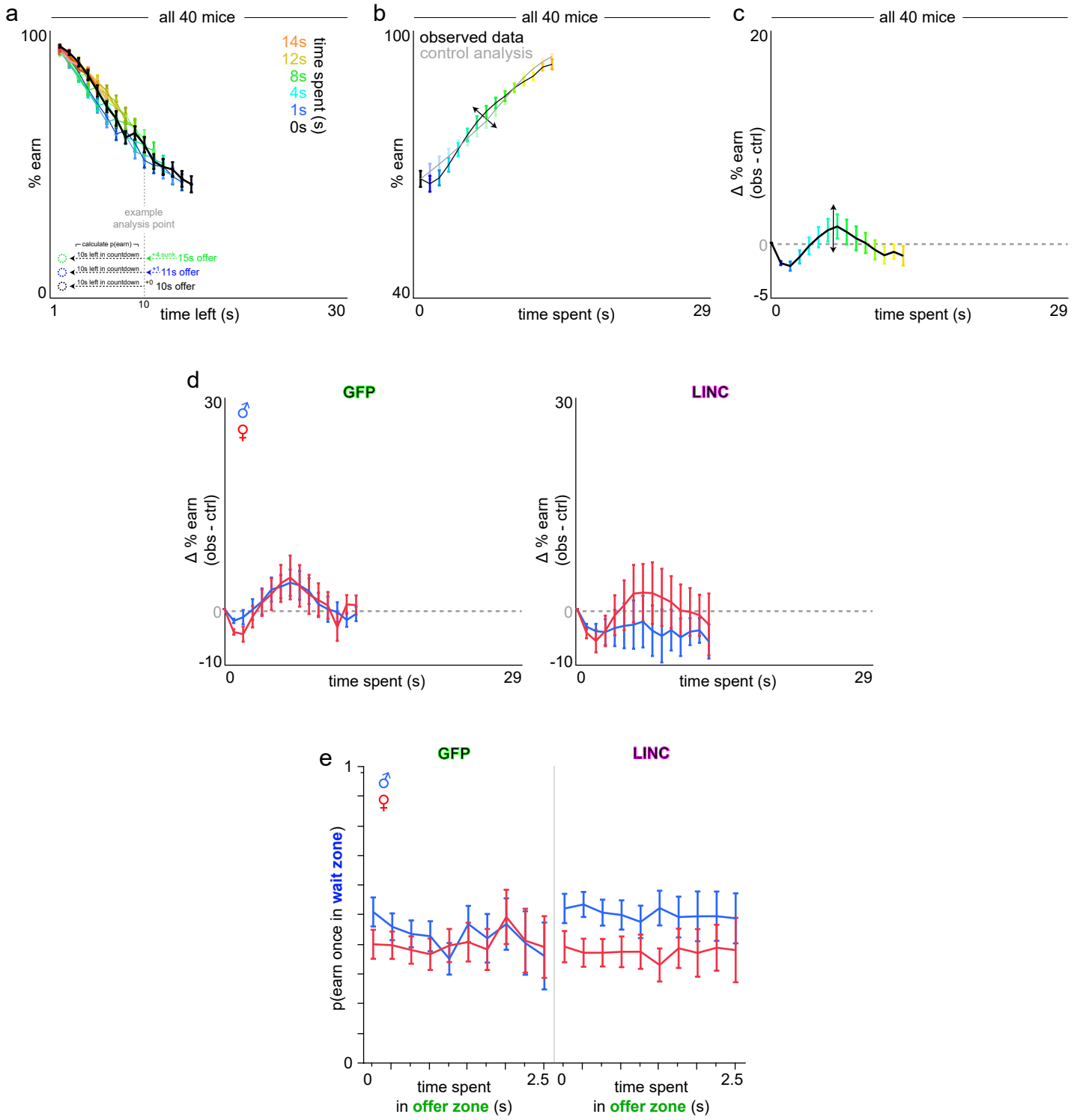
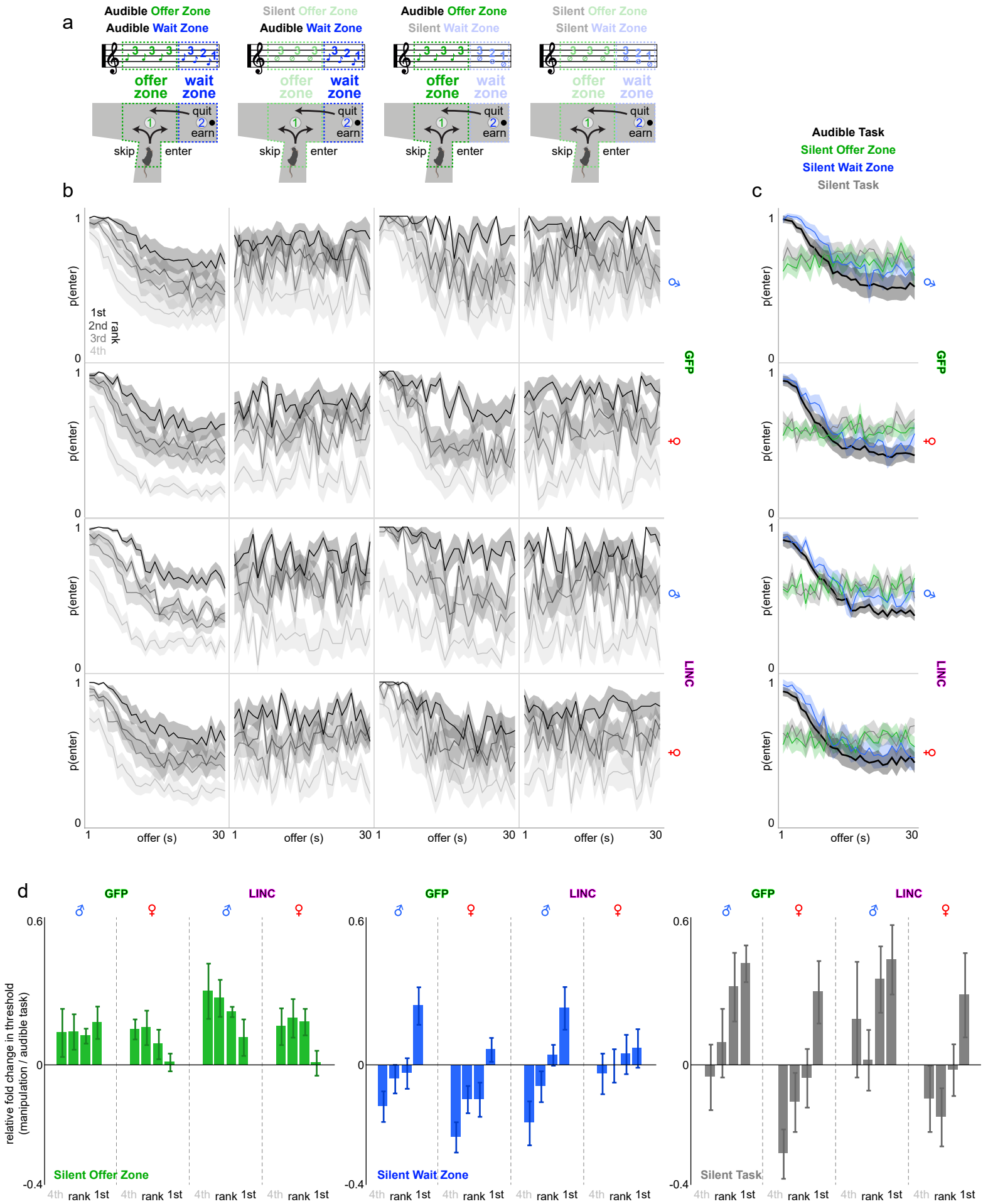
Supplementary Fig. 8